AD-A200 505

A TRIDENT SCHOLAR PROJECT REPORT

NO. 154

THE NONLINEAR INTERACTION OF TWO CROSSED FOCUSSED ULTRASONIC BEAMS IN THE PRESENCE OF TURBULENCE

UNITED STATES NAVAL ACADEMY
ANNAPOLIS, MARYLAND

UNCLASSIFIED

SECURITY CLASSIFICATION OF THIS PAGE (When Data Entered)

REPORT DOCUMENTATION PAGE		READ INSTRUCTIONS BEFORE COMPLETING FORM
1. REPORT NUMBER U.S.N.A. - TSPR: no. 154 (1988)	2. GOVT ACCESSION NO.	3. RECIPIENT'S CATALOG NUMBER
4. TITLE (and Subtitle) THE NONLINEAR INTERACTION OF TWO CROSSED FOCUSSED ULTRASONIC BEAMS IN THE PRESENCE OF TURBULENCE.		5. TYPE OF REPORT & PERIOD COVERED Final 1977/88 6. PERFORMING ORG. REPORT NUMBER
7. AUTHOR(s) Stephen C. Rife		8. CONTRACT OR GRANT NUMBER(s)
9. PERFORMING ORGANIZATION NAME AND ADDRESS United States Naval Academy, Annapolis.		10. PROGRAM ELEMENT, PROJECT, TASK AREA & WORK UNIT NUMBERS
11. CONTROLLING OFFICE NAME AND ADDRESS United States Naval Academy, Annapolis.		12. REPORT DATE 10 June 1988 13. NUMBER OF PAGES 64
14. MONITORING AGENCY NAME & ADDRESS(if different from Controlling Office)		15. SECURITY CLASS. (of this report) 15a. DECLASSIFICATION/DOWNGRADING SCHEDULE

16. DISTRIBUTION STATEMENT (of this Report)

This document has been approved for public release; its distribution is UNLIMITED.

17. DISTRIBUTION STATEMENT (of the abstract entered in Block 20, if different from Report)

18. SUPPLEMENTARY NOTES

Accepted by the U.S. Trident Scholar Committee.

19. KEY WORDS (Continue on reverse side if necessary and identify by block number)

Sound-waves
Scattering
Turbulence

20. ABSTRACT (Continue on reverse side if necessary and identify by block number)

This paper examines the scattering of a nonlinearly generated sum frequency acoustic wave component from a region of turbulence defined by the overlap volume of two mutually perpendicular crossed focussed ultrasonic beams. The scattered sum frequency pressure amplitude is measured at different radial scan positions across the jet flow stream providing conclusions that explain some qualitative results governing the sum frequency scattering mechanism.

(OVER)

DD FORM 1 JAN 73 1473 EDITION OF 1 NOV 65 IS OBSOLETE

S N 0102-LF-014-6601

UNCLASSIFIED

SECURITY CLASSIFICATION OF THIS PAGE (When Data Entered)

Information about the instantaneous velocity components of the turbulent field in the sound-sound interaction volume is measured with an electronic spectrum analyzer. Average spectral shapes of the spectrum near the sum frequency represent information about the probability distribution function of the turbulent velocities. Acoustic measurements are correlated with velocity measurements of circular jets that are well known and reported in the literature (Corrsin, Wygnanski). These correlations demonstrate that the focussed crossed beam apparatus is an effective diagnostic tool for the experimental study of turbulent fluid fields in water.

The focussed sound beams are generated by f_1=1.95 MHz and f_2=2.05 MHz frequency piezo-electric transducers. Each transducer has a one inch face and a six inch focal length. A mechanical apparatus supports the sending transducers above the water tank so that the position of the overlap region from the mutually perpendicular beams is varied across the width of the turbulence. The turbulence is produced by a submerged water jet of 9/32 inch diameter and nozzle exit speed of 15.6 m/s. The nonlinear scattered sound field of f = MHz is generated by the turbulent fluid field interacting with the overlapping sound field. An unfocussed transducer of resonant frequency 4 MHz (and 1 inch diameter face) is located 6 inches from the interaction region. The receiver is mechanically positioned such as that onscans across the interaction region the relative position of all three transducer units does not change. The acoustic signal received by the unfocussed transducer, which is proportional to an electronic voltage, is electronically processed by a spectrum analyzer. Sum frequency pressure measurements characterizing the instantaneous velocity structure of the turbulent-sound interaction volume are analyzed. An average spectrum of 20 trials per scan point provides information about the details of the probability density function of the turbulent velocities.

Plots of sum frequency acoustic pressure versus interaction position are presented and correlated with published and measured velocity profiles of a submerged water jet. The correlations indicate the scattering mechanism of the sum frequency wave results is not due to mean velocity components of the turbulent fluid field, but rather to the random fluctuating turbulent (rms) velocity components of the field.

The velocity structure of the turbulent flow is further described by statistical calculations of the scattered sum frequency pressure spectra. Measurements of the Skewness, S, and Kurtosis, K, of the pressure spectra give an indication as to the changing characteristics of the turbulent probability density function across the radial position of the turbulent jet. The statistical properties of Skewness, Kurtosis, and standard deviation, σ, of the received acoustic pressure are plotted vs position in the water jet.

The results of the nonlinear crossed beam experiments described herein indicate the apparatus can be utilized as a diagnostic tool to measure some parameters of turbulent velocity. The measured pressure of the radiated sum frequency correlates with turbulent velocities in the interaction region. Further, measurements of the Doppler shift and sum-frequency broadening are used to determine mean velocity and turbulent rms velocities respectively.

THE NONLINEAR INTERACTION OF TWO CROSSED FOCUSSED ULTRASONIC BEAMS IN THE PRESENCE OF TURBULENCE

A TRIDENT SCHOLAR PROJECT REPORT

BY

MIDSHIPMAN FIRST CLASS STEPHEN C RIFE, 1988

U.S. Naval Academy
Annapolis, Maryland

Associate Professor M. S. Korman Physics
Advisor Title/Rank and Name - Department

Professor J P Ulbrick
Co-advisor Title/Rank and Name - Department

Accepted for Trident Scholar Committee

Dennis F. Hesson
Chairperson

6/10/88
Date

USNA-1531-2

ABSTRACT

This paper examines the scattering of a nonlinearly generated sum frequency acoustic wave component from a region of turbulence defined by the overlap volume of two mutually perpendicular crossed focussed ultrasonic beams. The scattered sum frequency pressure amplitude is measured at different radial scan positions across the jet flow stream providing conclusions that explain some qualitative results governing the sum frequency scattering mechanism. Information about the instantaneous velocity components of the turbulent field in the sound-sound interaction volume is measured with an electronic spectrum analyzer. Average spectral shapes of the spectrum near the sum frequency represent information about the probability distribution function of the turbulent velocities. Acoustic measurements are correlated with velocity measurements of circular jets that are well known and reported in the literature (Corrsin, Wygnanski). These correlations demonstrate that the focussed crossed beam apparatus is an effective diagnostic tool for the experimental study of turbulent fluid fields in water.

The focussed sound beams are generated by f_1=1.95 MHz and f_2= 2.05 MHz frequency piezo-electric transducers. Each transducer has a one inch face and a six inch focal length. A mechanical apparatus supports the sending transducers above the water tank so that the position of the overlap region from the mutually perpendicular beams is varied across the width of the turbulence. The turbulence is produced by a submerged water jet of 9/32 inch diameter and nozzle exit speed of 15.6 m/s. The nonlinear scattered

sound field of $f_+ = 4.00$ MHz is generated by the turbulent fluid field interacting with the overlapping sound field. An unfocussed transducer of resonant frequency 4 MHz (and 1 inch diameter face) is located 6 inches from the interaction region. The receiver is mechanically positioned such as that onscans across the interaction region the relative position of all three transducer units does not change. The acoustic signal received by the unfocussed transducer, which is proportional to an electronic voltage, is electronically processed by a spectrum analyzer. Sum frequency pressure measurements characterizing the instantaneous velocity structure of the turbulent-sound interaction volume are analyzed. An average spectrum of 20 trials per scan point provides information about the details of the probability density function of the turbulent velocities.

Plots of sum frequency acoustic pressure versus interaction position are presented and correlated with published and measured velocity profiles of a submerged water jet. The correlations indicate the scattering mechanism of the sum frequency wave results is not due to mean velocity components of the turbulent fluid field, but rather to the random fluctuating turbulent (rms) velocity components of the field.

The velocity structure of the turbulent flow is further described by statistical calculations of the scattered sum frequency pressure spectra. Measurements of the Skewness, S, and Kurtosis, K, of the pressure spectra give an indication as to the changing characteristics of the turbulent probability density function across the radial position of the turbulent jet. The statistical properties of Skewness, Kurtosis, and standard deviation,σ, of the received acoustic pressure are plotted vs position in the water jet.

The results of the nonlinear crossed beam experiments described herein indicate the apparatus can be utilized as a diagnostic tool to measure some parameters of turbulent velocity. The measured pressure of the radiated sum frequency correlates with turbulent velocities in the interaction region. Further, measurements of the Doppler shift and sum-frequency broadening are used to determine mean velocity and turbulent rms velocities respectively.

TABLE OF CONTENTS

INTRODUCTION

The study of nonlinear acoustic wave propagation is complex. A history of its study is given by R. T. Beyer (Beyer). A nonlinear situation closely analogous to the propagation of a sound wave (a longitudinal disturbance) is the propagation of a transverse ocean wave. A linear model describing an ocean wave would predict a constant shape to the wave crest or trough as it travels across the ocean. Yet, anyone who has ever been to the beach knows a wave does change shape as it reaches the shore and breaks. Thus, a linear theory does not fully describe the propagation of an ocean wave. Similarly, a linear model does not accurately describe the propagation of a sound wave, or the interaction of one sound wave with another. For very low amplitudes, a sound wave shape will distort ever so slightly as it propagates. In most cases this small distortion is never considered for so called "infinitesimal amplitude" waves. When a sound wave of "finite amplitude" propagates its shape changes similar to the change in shape of the ocean wave. A shock is said to form when the distortions are at their greatest. When two sound beams cross and overlap the principle of superposition does not describe the crossing region completely. To completely describe sound, a nonlinear theory is necessary to describe the amplitude levels of distortion which are observed in the form of harmonics and combination frequencies that are generated from a pure acoustical tone.

As a sound wave travels, its shape distorts resulting in the growth of harmonics of its primary frequency. A listener down range from a sound source will not only hear the initial source frequency (called the

fundamental), but will also detect frequencies which are whole multiples of the source frequency (called harmonics). The intensity of those frequency components is usually much less than the fundamental.

Another physical phenomenon due to the nonlinearity of sound arises from the interaction of two sound beams. Nonlinear acoustic theory predictions by Westervelt in 1957 (Westervelt) claim the existence of a sum and difference frequency wave to exist only in the overlap region of two crossed finite-amplitude beams of frequencies f_1 and f_2. The sum frequency acoustic wave is a wave whose frequency is the sum of the frequencies of the two sound beams. Westervelt predicted that the sum and difference frequency components $f_+ = f_1 + f_2$ $f_- = f_1 - f_2$ can not propagate outside this interaction region. Late in the 1950's experiments by Smith and Beyer (Beyer) verified Westervelt's then controversial theory using crossed beams in water.

To appreciate the complexity of describing the nonlinear interaction of two crossed sound beams, one only need realize that as recently as 1960 top researchers in this field could not agree on their theoretical and experimental results on whether the sum and difference frequencies could radiate from the interaction region in a homogeneous flow. A history of the progress unraveling the controversy is given by Beyer (Beyer). Westervelt's general ideas stand correct. Experimentalists reporting sum frequency radiation measurements used scattering geometries that needed improvement.

Westervelt predicted that placing a solid object in the interaction volume would result in the propagation of sum and difference frequency sound beams outside the interaction region. Beyer and others performed

experiments using cylinders, spheres and bubbles in the interaction region and measured the radiated pressure.

In 1978 Westervelt suggested that another type of inhomogeneity, a turbulent fluid field, would also cause the scatter of sum and difference frequency sound waves from the interaction volume. Acting on Westervelt's suggestion Korman and Beyer quickly showed experimentally that a sum frequency is scattered from the interaction volume of two sound beams crossing in a region of turbulence in water. Angular measurements of the scattered sum pressure wave uncovered some structure to the average turbulent velocity field.

Korman and Beyer's sum frequency measurements used two mutually perpendicular sound beams overlapping and interacting (collimated fairly well) in the turbulence created by a submerged turbulent water jet. In this experiment the sound-sound turbulent interaction volume spanned the effective width of the jet. From the angular measurements, the mean and turbulent fluid particle velocities averaged over the width of the turbulent water jet were predicted.

The arrangement used for measurements described in this report uses focussed beams crossing at right angles for more spatial resolution. Focussing and crossing the sound beams makes the sound-sound interaction volume relatively small. By making this region small, acoustic measurements made can describe the turbulent and mean velocities of small volumes of fluid in the turbulent field. Thus, the acoustic measurements made in these experiments describe local fluid velocities at the crossing point.

With the added spatial resolution obtained by using crossed focussed sound beams, it was decided to make sum frequency acoustic measurements while scanning the interaction volume across the width of the turbulent water jet. The sum frequency pressure profile of the water jet turbulence can then be obtained and correlated with well known experimental data for the turbulent velocity field.

Goals of this research include mapping out the turbulence and studying the physical mechanisms responsible for the scattering of the sum frequency acoustic wave. Turbulent fluid motion will be described more fully in a later section, but for now it will be described as consisting of two parts -- an average or mean velocity, and added to that a random or turbulent velocity. By comparing scattered sum frequency pressure profiles to mean and turbulent velocity profiles, the scattering mechanism will be shown to be due to mean values or turbulent values of fluid motion.

Calculations from the sum frequency acoustic pressures are used to produce an average sum frequency pressure profile of the turbulent jet at a cross section 30 nozzle diameters from the 9/32 inch jet outlet nozzle. The results of four different runs are presented. These profiles are curve fitted to four curve forms. The curve forms chosen often are used by turbulence researchers to fit mean and turbulent velocity profiles.

Statistical calculations are also made of the scattered sum frequency pressure spectrum. Values of Skewness and Kurtosis are determined from treating the spectra as a probability distribution of scattered sum frequency pressure.

Doppler shifting and frequency broadening of the scattered sum

frequency acoustic wave in the received spectrum can be related to mean flow velocity and rms turbulent velocities respectively.

Results of pitot tube measurements used to determine the mean velocity profile of the turbulent jet at the same cross section as the acoustic scans are also graphed and presented.

THEORETICAL DEVELOPMENT OF THE INTERACTION OF SOUND WITH TURBULENCE

Understanding the physical interactions involved in the nonlinear crossed beam scattering experiment requires accurately describing the fluid fluctuations in the sound - sound - turbulence interaction volume. The interaction volume can be described as consisting of three fluctuating fluid sources -- the two primary sound beams, and the highly dispersive turbulent field as shown in Fig 1. Lighthill's aerodynamic theory used to explain sound generated by turbulent fluid motion (such as that generated by the turbulent exhaust of a jet engine) can be used to describe both sound and turbulent velocity fluctuations in a volume of fluid flow. His equation is especially suited to describe the interaction of sound with turbulence and thus becomes the starting point for the theoretical description of this physical interaction.

Lighthill's equation in tensor form is:

$$\frac{\partial^2 \rho}{\partial t^2} - c_0^2 \frac{\partial^2 \rho}{\partial x_i} = \frac{\partial Q}{\partial t} - \frac{\partial F_i}{\partial x_i} + \frac{\partial^2 T_{ij}}{\partial x_i \partial x_j}$$

where

$$T_{ij} = \rho u_i u_j + (P - c_0^2 \rho)\,\delta_{ij} - \eta_{ij}$$

defines Lighthill's stress tensor, and δ_{ij} is the Kronecker delta.

Here ρ is the density, p is the pressure, u is the fluid particle velocity field, Q is the rate of introduction of new fluid mass into a unit volume, F is the external force per unit volume, P_o is the ambient pressure, c_o is the small

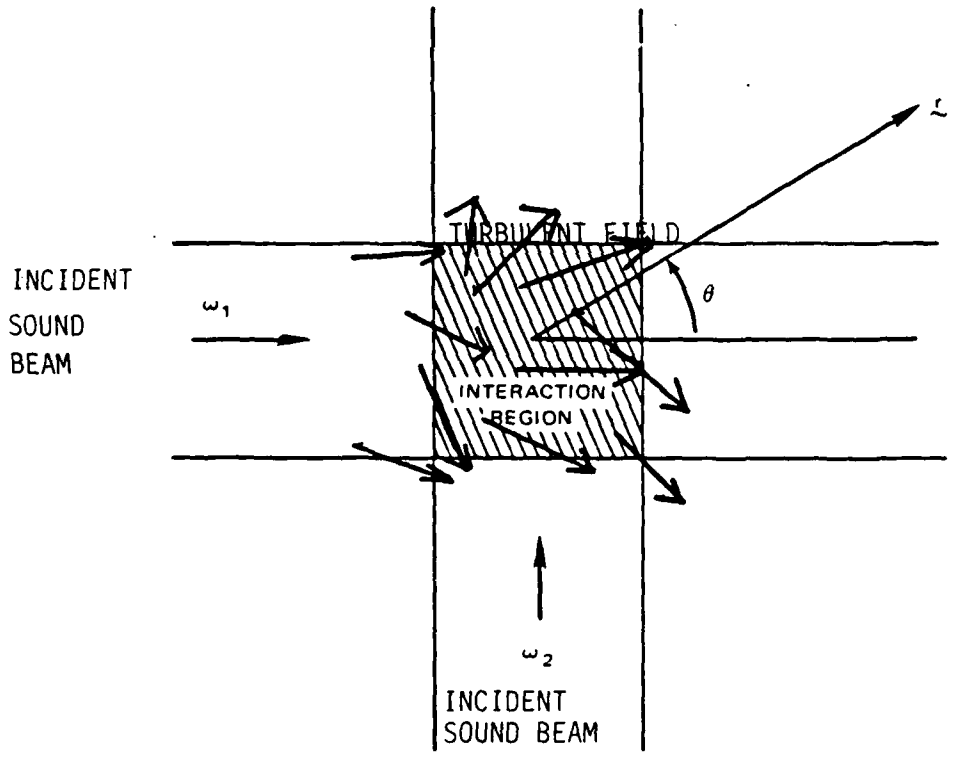

FIG 1: Geometry for the interaction of two sound beams in turbulence. (ref. Beyer)

amplitude speed of sound in the absence of turbulence, and t is the time. The Cartesian coordinates are x_i(i=1, 2, 3), $u_i(\underset{\sim}{x},t)$ is the velocity field and $\rho(\underset{\sim}{x},t)$ is the density. Viscous stress terms are represented by τ_{ij}.

Using a perturbation theory in the Lighthill Equation Korman and Beyer (Korman 1981) described the nonlinearly scattered sum frequency wave component.

The fluid particle velocity field $u_i(x,t)$ is resolved into an acoustical or longitudinal part from the velocities of the incident sound beams $\underset{\sim}{u}_i^{(L1)} + \underset{\sim}{u}_i^{(L2)}$ and a shear or transverse part $u_i^{(T)}$ from the turbulence.

The combined known velocity fields are then taken to be

$$\underset{\sim}{u}_i(x,t) = u_i^{(L1)} + u_i^{(L2)} + u_i^{(T)}$$

and the combined known density field is

$$\rho(x,t) = \rho_0 + \rho_1 + \rho_2$$

The dominant scattering term is given by the expression below:

$$\rho_{s+} = -\frac{2\rho_0}{4\pi c^2} \int \frac{\partial^2 \left\{ \left[(\rho_1/\rho_0) u_i^{(L2)} + (\rho_2/\rho_0) u_i^{(L1)} \right] u_j^{(T)} \right\} d^3\underset{\sim}{y}}{\partial y_i \, \partial y_j}$$

where the term in braces is given at the retarded time $\tau = t - |\underset{\sim}{x} - \underset{\sim}{y}| / c$

An ensemble average spectrum of the scattered sum frequency intensity is given by,

$$\left\langle I_s^{(+)}(\underset{\sim}{x}, \omega) \right\rangle = \frac{c^2/\Delta T}{(1\ m/s)^2} \frac{\pi (\omega^4/c^8)}{16} \left(m_{01} m_{02} C\right)^2 \left[\left(n_i^{(\omega)} + n_i^{(\omega 2)} \right) \eta_j \right]^2$$

$$\times \left[1 - (\underset{\sim}{\eta} \cdot \underset{\sim}{K}_+)^2 / K_+^2 \right] F\left(|K_+|, |\omega| - \omega_0^+ \right)$$

where

$m_{o_1} = u_{o_1}/c$, $m_{o_2} = u_{o_2}/c$, $\underset{\sim}{K}_+ = \underset{\sim}{K}_1 + \underset{\sim}{K}_2$, $K_+ = |K_1 + K_2|$

The quantities

$\underset{\sim}{K}_1 = K_{o_1}(\underset{\sim}{n} - \underset{\sim}{n}^{(o_1)})$, $\underset{\sim}{K}_2 = K_{o_2}\langle \underset{\sim}{n} - \underset{\sim}{n}^{(o_2)} \rangle$, $K_{o_1} = \omega_{o_1}/c$, $K_{o_2} = \omega_{o_2}/c$

represent scattered wave vectors where n is the scattered direction (a unit vector) and $\underset{\sim}{n}^{(o_1)}$ and $\underset{\sim}{n}^{(o_2)}$ are the incident directions of the beams. $F(K, \omega)$ is the 4 dimensional space-time spectral density of isotropic turbulence fluctuations given by $F(K,\omega) = |\hat{u}_i^{(T)}(\underset{\sim}{K}, \omega)|^2$

Here $\hat{}$ denotes a Fourier transform over space and the finite time interval ΔT, and $\langle\ \rangle$ denotes an ensemble average.

The total scattered intensity is obtained by integrating over the band of frequencies near the sum frequency. This result is given by

$$\langle I_s^{(+)}(\underset{\sim}{x}) \rangle = \int \langle I_s^{(+)}(\underset{\sim}{X}, \omega) \rangle \, d\omega .$$

Korman and Beyer showed that for certain Gaussian statistics of the turbulent velocity field the Doppler shift in the sum frequency spectrum is given by

$$\omega_d^{(+)} = 2\pi f_d^{(+)} = -\underset{\sim}{K}_+ \cdot \underset{\sim}{V}_o$$

where $\underset{\sim}{V}_o$ is the mean velocity vector of the flow.

For the crossed beam arrangement of this paper, f_d is given by

$$f_d = \frac{1}{2\pi} \frac{\sqrt{2}}{2} \frac{V_o}{c} \left[|f_{o_1} - f_{o_2}| \cos\theta_* + |f_{o_1} + f_{o_2}| \sin\theta_* \right]$$

The angle θ_* is zero for the forward direction. Here f_{o1} and f_{o2} are the primary frequency components.

The sum frequency broadening of the intensity spectrum $\Delta f_e^{(+)}$ due to the fluctuations in the turbulence over time is defined to be the full width of the spectrum at the 1/e down point. The amount of broadening is given by

$$\Delta f_e^{(+)} = 4\,(2^{-1/4})\,(f_o^{+})\,(\sigma_v/c)\left[\sin^2(\theta_*/2) + 0.0303\right]^{1/2}$$

where σ_v is the rms velocity fluctuation of the turbulence that is taken to be isotropic.

Fig 2 shows a generated sum frequency waveform, and its Doppler shifted and broadened waveform. Although a Doppler shift of a wave exists even in a nonturbulent flow field, broadening, which occurs due to fluctuating Doppler shifts would not exist without a turbulent field. Broadening of the waveform occurs because the instantaneous velocity in turbulent fields is random. Thus the sum frequency acoustic wave is Doppler shifted random values depending upon the instantaneous velocity. By measuring pressure amplitudes of the scattered sum frequency as a function of frequency, as performed by a slowly sweeping spectrum analyzer, the broadened waveform can be measured. Since the shape of the spectrum can then be related to the shape of a probability density distribution of instantaneous fluid velocities in the interaction region, emphasis should be made that Korman and Beyer's Doppler and broadening formulas are only

accurate for Gaussian shaped turbulent velocity profiles.

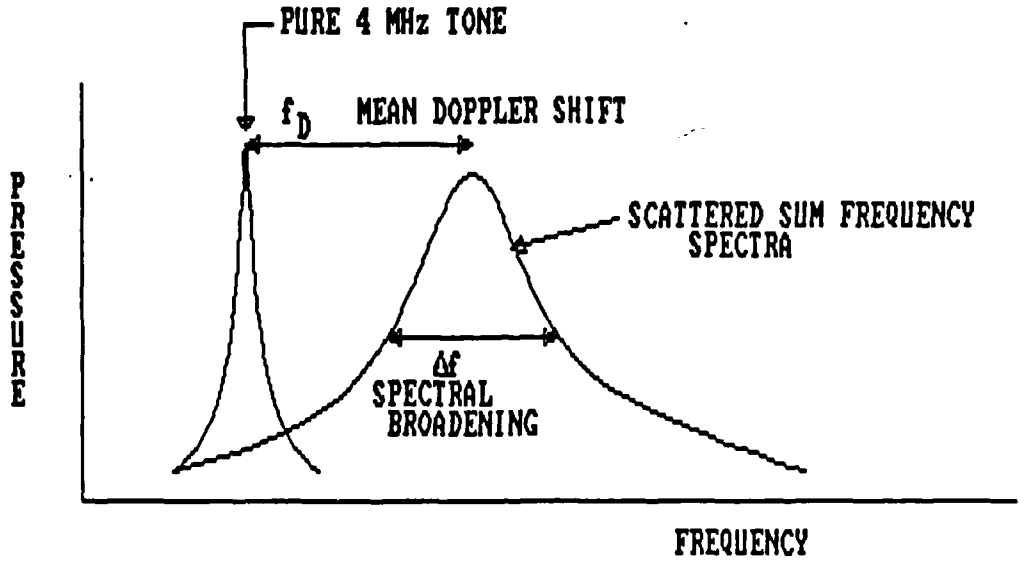

FIG. 2: DOPPLER SHIFTED AND BROADENED SPECTRA

DISCUSSION OF TURBULENCE

Fluid velocities in a fluid jet are currently determined from measurement devices such as pitot tubes, hot film anemometers, and laser-Doppler anemometers. Because of the randomness and complexity of the fluid motion, though, no accurate theoretical models are known which can predict the fluid motion. Randomness characterizes turbulence. Hinze (ref) defines turbulent fluid motion as "an irregular condition of flow in which the various quantities show a random variation with time and space coordinates, so that statistically distinct average values can be discerned."

A statistical approach to describing turbulent motion is thus preferred over a deterministic approach. A statistical approach taken is to make measurements of instantaneous velocities at a point in the fluid field, and to plot the percentage of times the velocity is a certain value vs that value. This plot is called a probability density distribution of fluid velocity. Fig 3 shows a probability density distribution, with velocity values that were previously measured as a function of time.

The shape of the probability density distribution B(u) is described by various statistical parameters. The first moment or mean value is defined by

$$U \equiv \int_{-\infty}^{\infty} u\, B(u)\, du$$

In experimental work, the mean velocity U is always subtracted from the fluctuating turbulent velocity u. Fluctuations are denoted by u', so that $u' = u - U$ and $\bar{u} = 0$.

The mean-square departure σ^2 from the mean value U is called the

variance, or second moment, and is defined by

$$\sigma^2 \equiv \overline{u'^2} = \int_{-\infty}^{\infty} u'^2 B(u')\, du'$$

The square root of the variance is the standard deviation. The standard deviation is a measure of the width of B(u).

Although the standard deviation gives a range of values describing the width of the probability density distribution, it provides no information on symmetry. The third moment, however, defined by

$$\overline{u_3'} \equiv \int_{-\infty}^{\infty} u'^3 B(u')\, du'$$

describes the asymmetry in B(u). Skewness is the nondimensionalized third moment, and is defined as

$$S \equiv u'^3/\sigma^3$$

Fig 3 shows a probability density distribution with positive Skewness. The Skewness is positive because large negative values of velocity are not as frequent as large positive values of velocity. Skewness is a measure of the anisotropy of turbulent eddies and velocity gradients in turbulent flow.

The fourth moment, Kurtosis or flatness, also provides information about the shape of B(u). Kurtosis is also nondimensionalized and defined as

$$K \equiv \frac{\overline{u'^4}}{\sigma^4} = \frac{1}{\sigma^4} \int_{-\infty}^{\infty} u'^4 B(u')\, du'$$

A comparison of Kurtosis for different functions is sketched in Fig 4. A large Kurtosis is seen to correspond to functions which vary dramatically from one reading to the next. Thus values of B(u') out on the skirts become

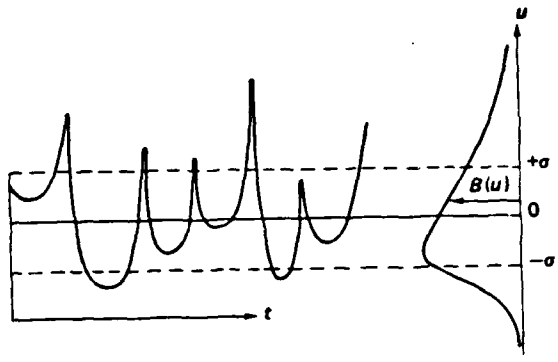

Figure 3: A function with positive skewness.

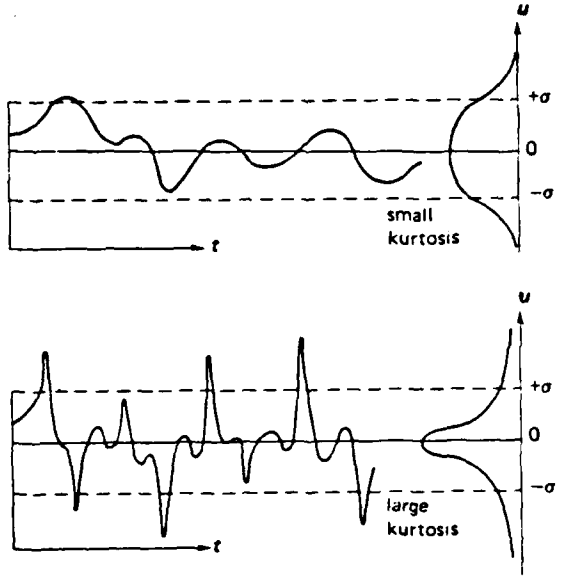

Figure 4 : Functions with small and large kurtosis.

(ref. Tennekes and Lumley)

relatively large for a jet flow. Intermittency, or the sporadic bursting of turbulence in time followed by a duration of nonfluctuating velocity, is a pattern of flow that can be characterized by Kurtosis.

The probability density distribution of fluid velocity at a point in the water jet can be related to the nonlinear pressure spectra generated for that point in the flow. Measurements of Skewness and Kurtosis values from radial scans of the spectra across the jet should be related to the characteristic turbulent velocity changes in S and K across the jet.

The turbulence chosen to generate the fluid field is a relatively simple type of flow to create in the laboratory and to control. Its other advantage is the high ratio of turbulent velocity to mean velocity u'/U, which reaches 0.3 at certain radial positions in the jet. Turbulent velocities are suspected to be responsible for the sum frequency scattering according to the Korman-Beyer theory. High values of turbulence are desired. Additionally, this type of turbulence has been studied extensively and is available in research journals on fluid mechanics, so data on fluid velocities is readily available.

A schematic of a circular turbulent jet is sketched in Fig 5. The jet boundary marks the edge of the zero velocity field. Downstream from the nozzle (at roughly 30 - 50 nozzle diameters), the jet reaches fully developed flow. In the region of fully developed flow the velocity profiles at various cross-sections do not depend on the Reynolds number, $Re=\rho Ud/\mu$, of the jet. Here U is the nozzle exit velocity, d is the nozzle diameter, μ is the viscosity of the fluid, and ρ is its density. Experimental studies (Hinze, Tennekar & Ludy, Townsend) indicate the laminar jet becomes turbulent provided the Reynolds number is greater than about 200. The Reynolds number for these

experiments is 17000. Plots of normalized velocity u/u-max vs normalized radial position r/Z, where Z is the distance from the outlet nozzle to the cross section of measurement are shown to be the same for all cross sections in the fully developed regime of flow. Thus, since scattered sum frequency pressure is related to velocity, normalized pressure profiles at various scan cross sections should also be equal.

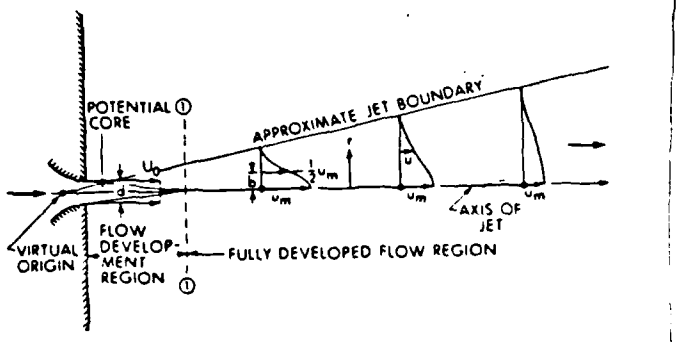

Fig 5a: Definition sketch of circular turbulent jets (ref. Abramovich, G. N., The Theory of Turbulent Jets, Copyright 1963 by the MIT Press)

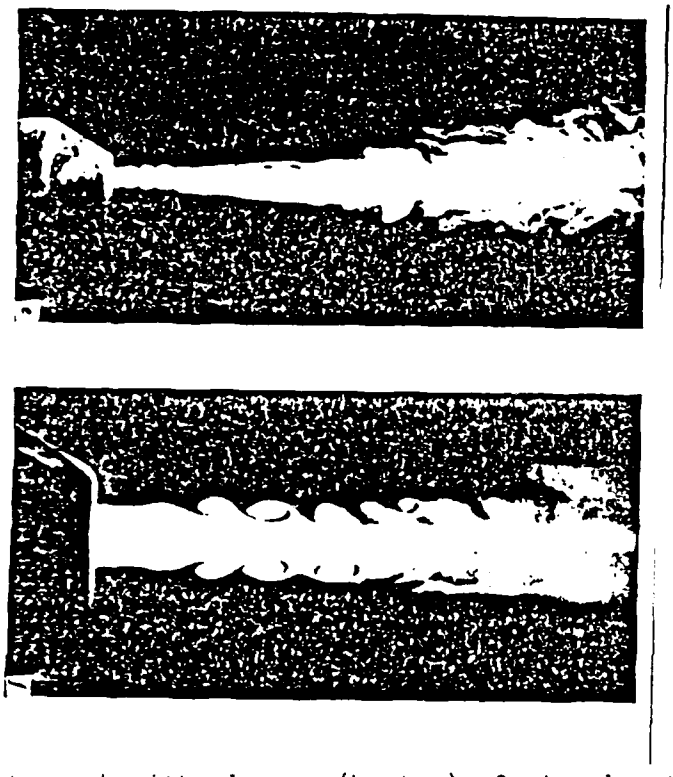

Fig 5b: Photograph with closeup (bottom) of circular turbulent jet (ref. Becker, H. A. and T. A. Massaro, "Vortex evolution in a round jet", J. Fluid Mech. (1968), vol. 31, part 3, p. 448)

EXPERIMENTAL ARRANGEMENT

The major development of this crossed beam arrangement over the previous one used by Korman and Beyer is to create a much smaller sound-sound interaction volume through the use of focussed acoustic beams, crossing at right angles to each other. The sound sources (piezo-electric transducer units of one inch diameter) are accurately aligned to form an interaction volume at the focus. This was done with a mechanical apparatus which had positioning equipment for translation and rotation.

The geometry of the acoustic beams and turbulence, shown in Fig 6 is now discussed. A small tank was chosen so that the crossed beam arrangement could fit into a small lab (Michelson Hall Lab A8). Focal lengths of six inches are were chosen for each of the focussed sending transducers which generated 1.95 and 2.05 MHz continuous wave (C.W.) acoustic waves respectively. The beams are chosen to cross at right angles to conform to the previous experiment of Korman and Beyer. The interaction volume is also minimized for beams overlapping at 90^{o}. The receiving transducer axis bisects the angle defined by the axes of the focussed transducers. It is located at the same depth as each sender. The unfocussed receiving transducer is also located six inches from the interaction volume.

The transducer positions also are chosen so that the units will not interfere with the jet flow when scanning. At 30 nozzle diameters from the jet outlet nozzle, the width of the jet is approximately four inches. The radial distance from the interaction volume to the transmitting transducers is

greater than that, 4.25 inches, so they do not disturb the flow.

An enlargement of the acoustic geometry is shown in Fig 7. The interaction volume is approximately a few wavelengths of sound on a side.

A submerged underwater jet of inside diameter 9/32 inch and nozzle exit speed, U_{nozzle} = 15.6 m/s with a circular orifice creates the turbulence. At 30 nozzle diameters from the jet axis on axis, U= 2.5 m/s from pitot tube measurements, and u' is known to be 0.3 times that for a submerged water jet. A plumbing system necessary to produce adequate flow uses a 3/4 H.P. water pump with 1 1/2 inch diameter suction and discharge ports. For the purpose of reducing the turbulence in the pump and the pumping lines leading to the nozzle exit, a plenum with honeycomb and flow straighteners was designed. Fig 8 shows the major components in the water jet system.

The pump is throttled by a globe valve to produce a jet with a steady outlet nozzle velocity which was measured by a pitot tube and pressure gauges. The suction inlet opposite the outlet nozzle in the tank is positioned on the axis of the jet to reduce the effects of the flow deflecting off the back wall of the tank and producing a wall jet.

The major component in the system, the plenum, shown in Fig 9, is designed and built specifically for this project. Its purpose is to straighten the incoming flow at the outlet of the 9/32" diameter nozzle. Before the water enters the plenum, it is turbulent due to the piping system and pump. When fluid enters the plenum, its speed is decreased to dissipate turbulence. Next the flow is straightened by the honeycomb material in the plenum. A screen shields tiny turbulent vorticities which decay rapidly before flow exits out the nozzle. From this design, the exit flow more closely reaches a laminar

condition.

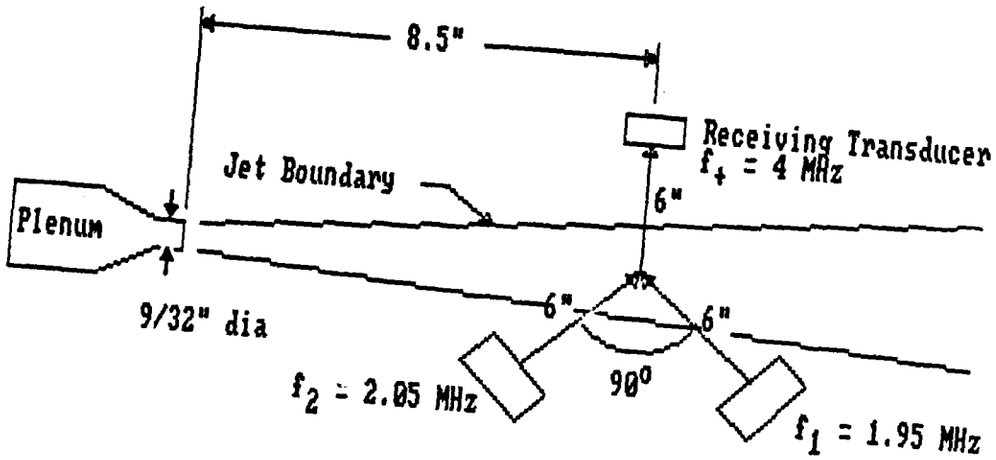

TOP VIEW

Fig 6: CROSSED BEAM GEOMETRY

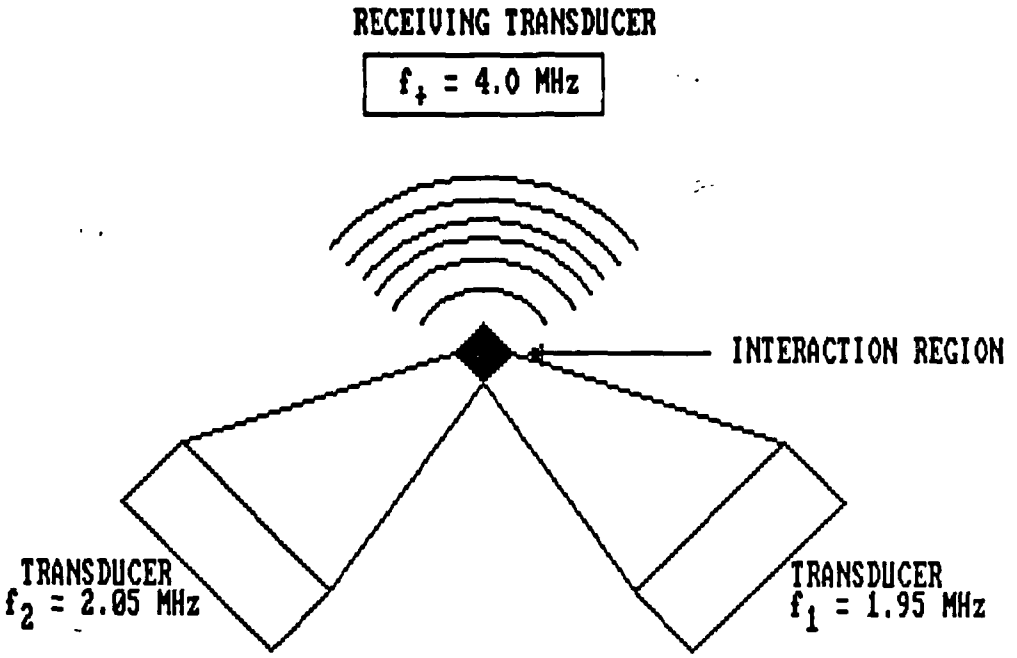

FIG. 7: CLOSE-UP OF CROSSED BEAM GEOMETRY

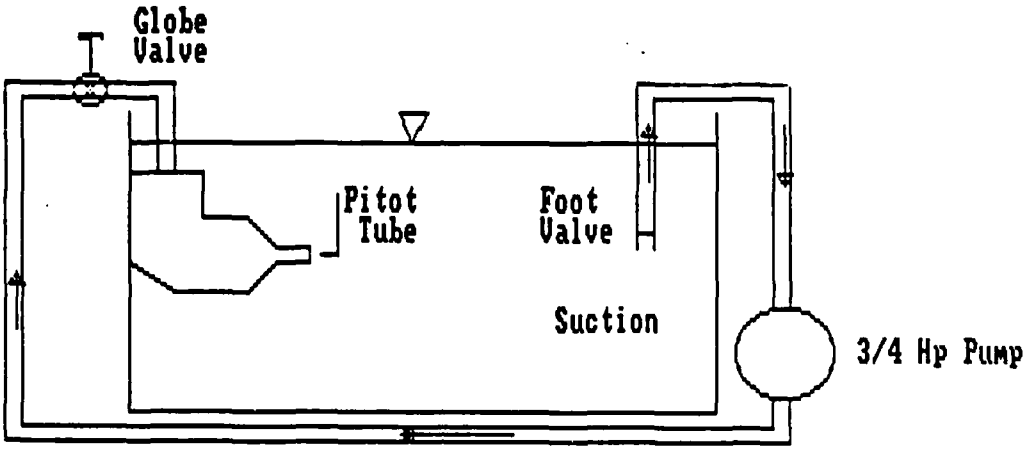

Fig 8: **Water Tank System**

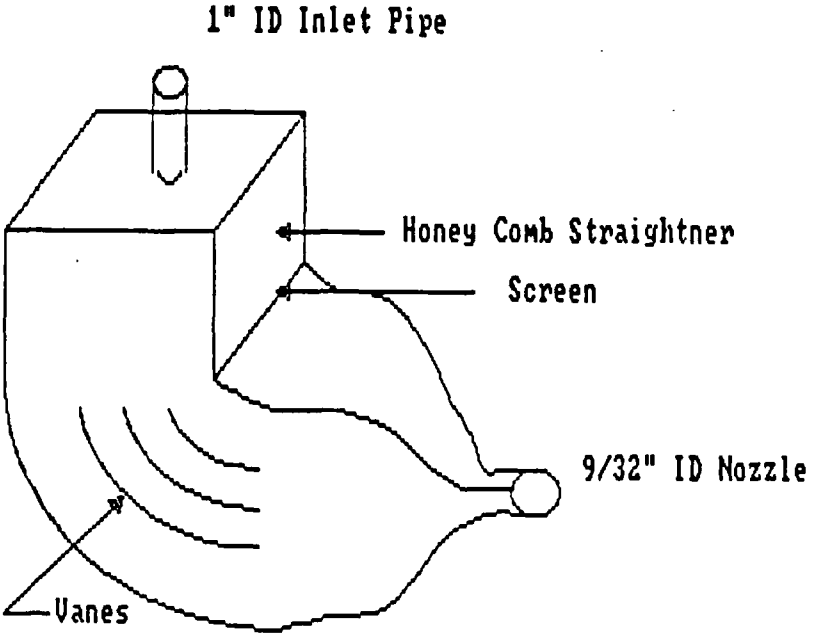

Fig 9: **PLENUM**

ELECTRONICS

The production of sound in air or in water or any fluid medium can be obtained by the vibration of a solid body in the fluid, such as the vibration of a vocal chord or guitar string. In this experiment a pure frequency, or in musical terms, a pure note of different frequency is needed from each of the crossed beam sources. The vibrating membrane chosen for the sound sources is the piezoelectric transducer. The heart of the piezoelectric transducer is the piezoelectric crystal, which deforms when a voltage drops across it. The sinusoidal voltage (at a constant frequency), deforms the crystal thickness at the same frequency resulting in an acoustic pressure which is generated at the transducer face and then propagates away. The transducer material is shaped in the form of plano-concave face with a radius of curvature needed to produce a six inch focal length for the sound beam in water.

A sinusoidal voltage at constant frequency, constant amplitude, and pure sinusoidal shape requires the construction of an elaborate electronic system. To produce a clean C.W. constant amplitude signal within frequency and no-drift, the electronics system shown in Fig 10 is used. The crystal oscillator in the system generates a sinusoidal signal. The signal passes through a low pass and a high pass filter. These filters eliminate electric signals of frequency lower than 1.75 MHz and higher than 2.55 MHz, thus reducing distortion in the signal. A matching network is placed after the power amplifier to match the rf. power into the ultrasonic transducer which is

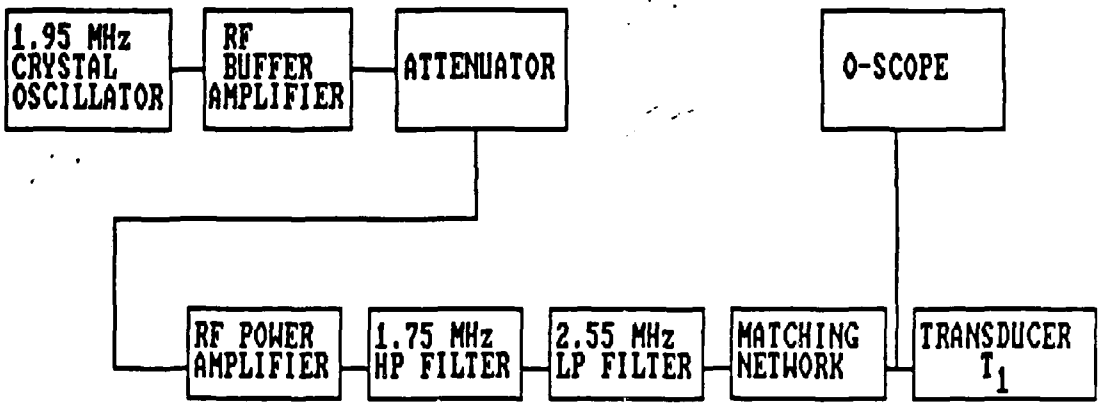

FIG. 10: TRANSMITTING ELECTRONICS FOR THE 1.95 MHz SOUND BEAM

considered the load.

The sum frequency component generated in the experiment radiates in all directions. Part of the energy of this scattered sound is captured by a receiving transducer positioned six inches from the interaction region. This receiving transducer crystal detects the sound impacting on it. The electric signal from the transducer carries all the information of the sound averaged over the transducer face. This signal is filtered for 4 MHz detection and amplified. It is then measured with a Tektronix 7L5 spectrum analyzer. The vertical and horizontal sweep is digitized on the Apple IIe computer scope to obtain an average sum frequency pressure spectrum as a function of frequency. The electronics which process the received signal are shown in Fig 11. The spectrum analyzer shown in Fig 12 sweeps through a range of frequencies using a variable bandpass filter to sample signal amplitudes. The resolution of frequency sampling window of the bandpass filter can be adjusted as well as the frequency window through which the filter sweeps The high resolution of the spectrum analyzer is used to process the Doppler shifted and broadened sum frequency spectra. The Apple IIe Computer Scope interfaced to the analyzer does the necessary computations. A program written by Dan Magsig averages 20 sum frequency spectra and stores the digitized values on disk. Statistical calculations of the spectra, including Skewness and Kurtosis, are then made. The intensity can be obtained by squaring the spectrum and integrating over all frequencies. The time required to average 20 spectra corresponding to one position of the interaction region in the flow is approximately 20 minutes. Thus, a scan of the jet at 0.2 inch intervals requires a minimum of seven hours to fully map

out a cross section of a four inch total width jet.

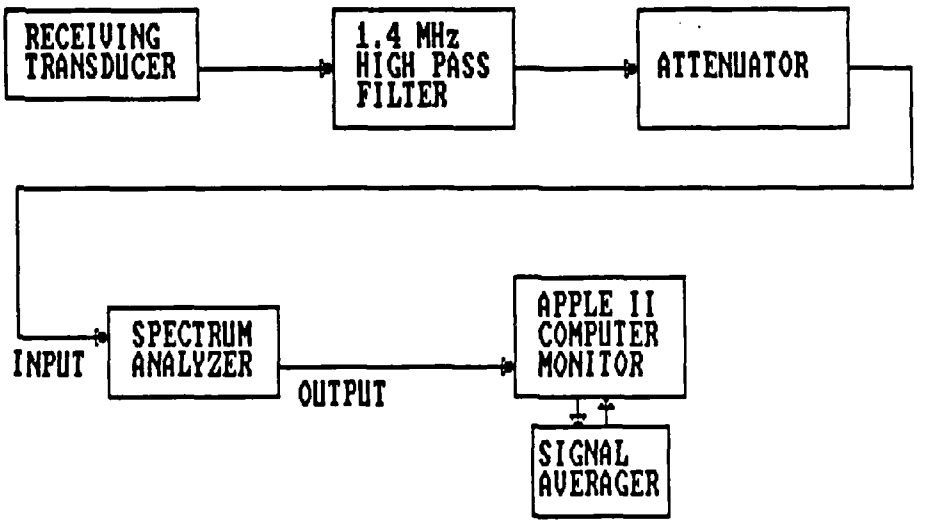

FIG. 11 RECEIVING ELECTRONICS

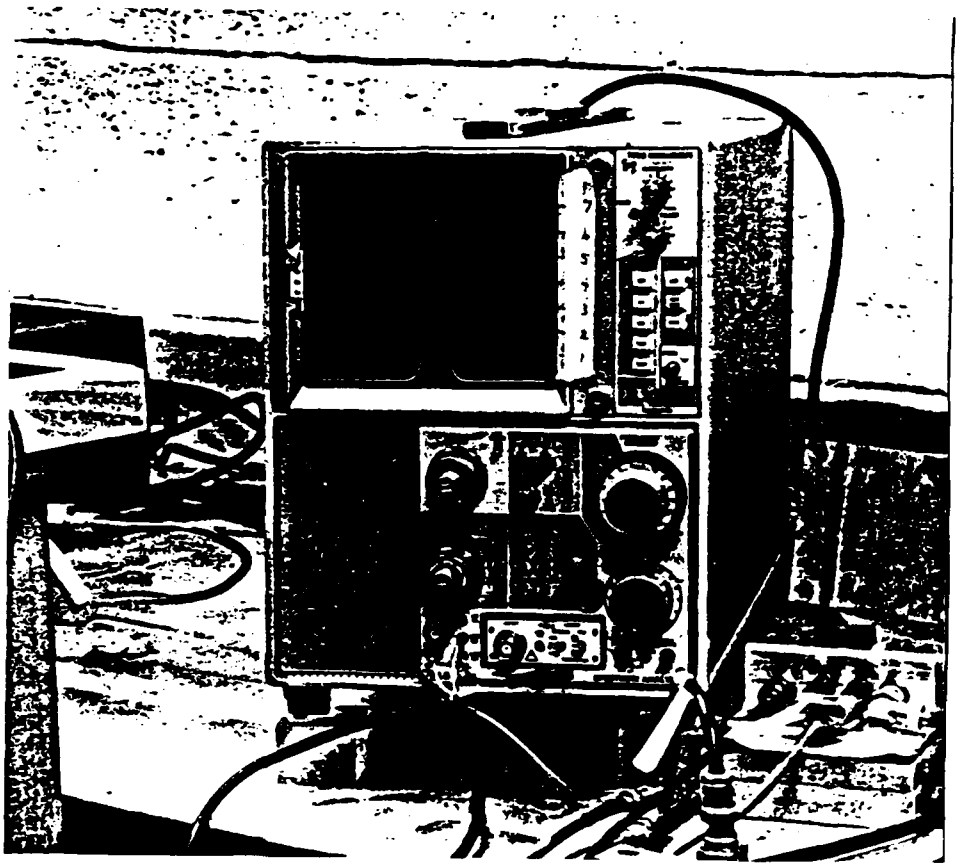

Fig 12: Tektronix 7L5 Spectrum Analyzer

NONLINEAR SCATTERING EXPERIMENTAL RESULTS

The measurements presented in this section map out the fully developed region of the water jet 30 nozzle diameters from the outlet nozzle. The jet outlet velocity is kept at 15.6 m/s corresponding to a Reynolds number of 17000 for all measurements made. The scans measure the scattered sum frequency pressure. Two types of measurements using different resolutions on the spectrum analyzer are used for the pressure measurements.

The first set of results is calculated from measurements using a low frequency resolution to capture the scattered sum frequency pressure over a wide frequency band. The data graphed are calculated from 25 pressure values corresponding to each data point. Two experimental runs of this type are shown for each graph.

Fig 13 shows the normalized average sum frequency scattered pressure plotted vs normalized radial position in the jet. The pressure values are low at the edges of the turbulent jet and high near its axis. This behavior agrees with velocity measurements across the jet. The pressure profile is symmetric about the jet axis. Two experimental methods are used to calculate the pressure measurements. One method reads cursor values off the Apple Computer Scope that captures data at a very fast sweep rate, allowing the sweep rate of the analyzer to be very fast. This corresponds to looking at the pressure spectrum at very low frequency resolution. The second method involves recording data directly off the vertical scale of the analyzer which requires the sweep rate to be somewhat slower and the resolution to be somewhat higher. The second method serves as a check and agrees very well

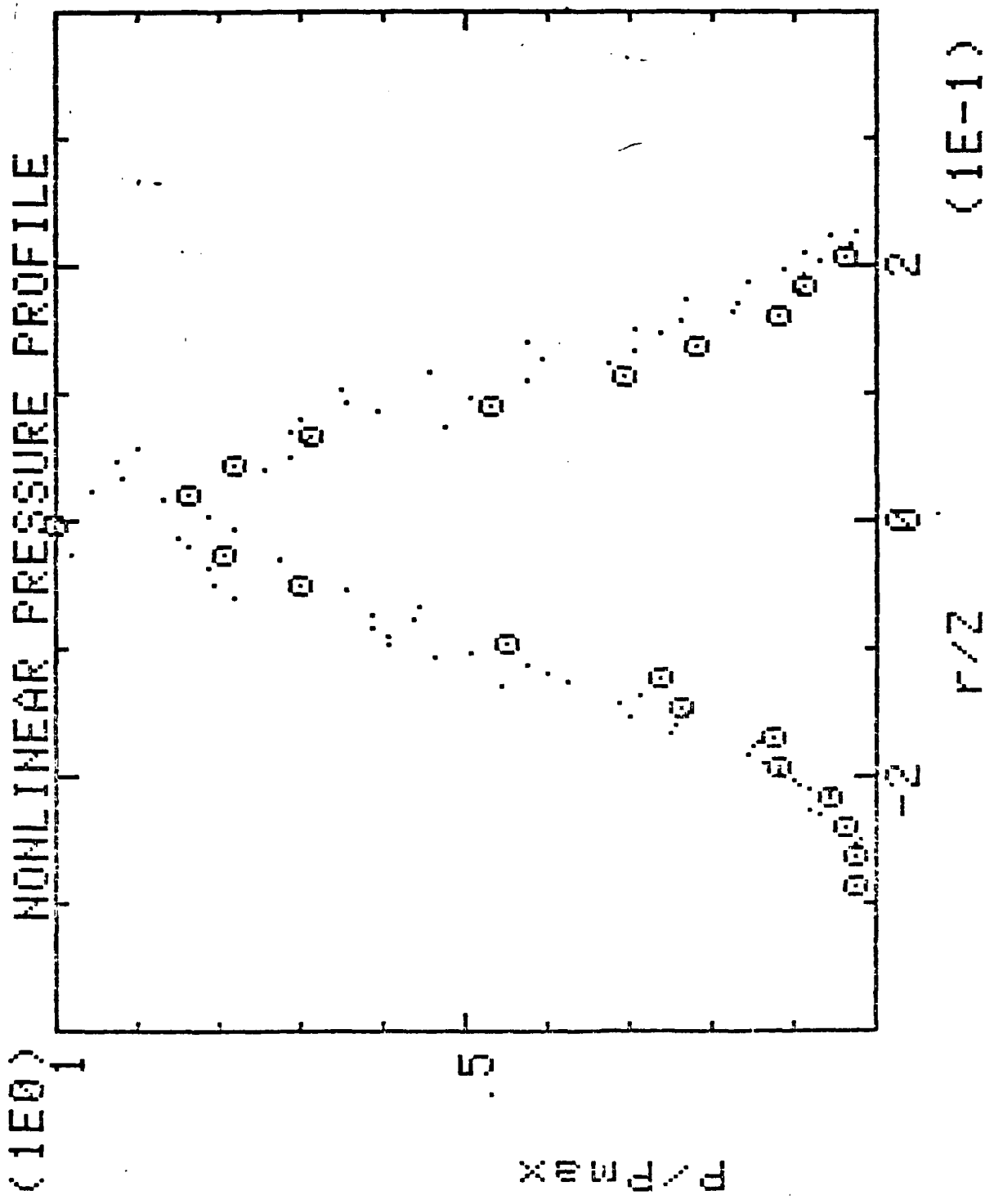

Fig 13: Nonlinear pressure profiles using low resolution frequency sampling
(Data points corresponding to two different data runs)

with the more precise first method.

Results measuring the scattered sum frequency pressure spectra are presented first These measurements are generated using a high resolution or small bandwidth on the spectrum analyzer to detect broadening and Doppler shift in the sum frequency spectra. The high resolution reduces the sweep rate on the spectrum analyzer as it samples small frequency increments around the 4 MHz sum frequency. A scattered spectrum is shown in Fig 14. The pressure spectra are generated from ensemble averages taken from 20 sweeps through the sum frequency spectra range. These spectra are digitized, squared, and then processed to calculate values of standard deviation in frequency (or spectral broadening), Skewness, and Kurtosis from the intensity spectra.

Relative root-mean-square pressure values are obtained from the intensity spectra by integrating intensity over differential frequency steps, and taking the square root of the intensity. These results are plotted across the width of the jet in Fig 15. Results of two different scans show repeatability of the measurements. Repeatability is significant for this case since all transducers were realigned for the second scan. The sum frequency root mean square pressure profile shows low values of pressure at the edges of the jet and high values at the center. The profile is smooth and symmetric about the axis of the jet suggesting good correlation with velocity profiles of the jet.

A further correlational study comparing sum frequency pressure profiles to turbulent and rms velocity profiles is given in detail in Appendix B. Results comparing fitted constants of velocity profile curve forms for pressure and velocity data indicate conclusively that the scattering of the sum

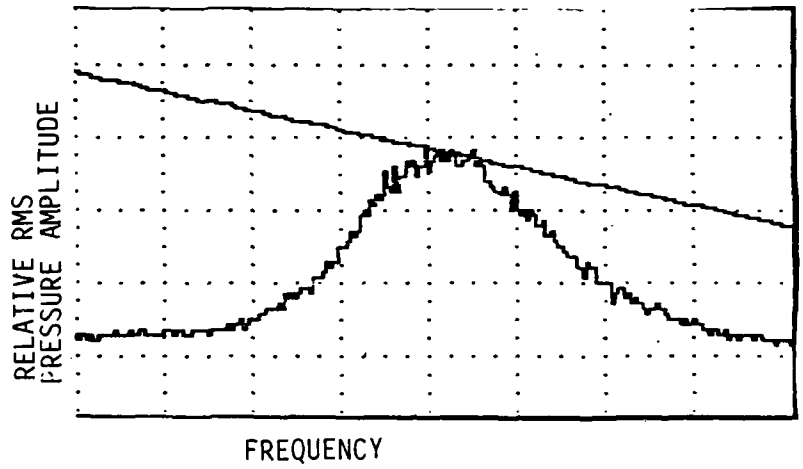

Fig 14: Scattered sum frequency spectrum

frequency wave is due to turbulent velocity components not mean velocity components.

Values of Skewness and Kurtosis from intensity spectra are next presented in Fig 16. The plot shows repeatability for both Skewness and Kurtosis. The Skewness at the center to half width of the jet is negative, and becomes positive at the edges of the jet. Skewness is symmetric about the center of the jet. Kurtosis, too, is symmetric about the center of the jet, and shows high values at the center. A sharp drop off of Kurtosis is seen at r/Z values at + or - 0.6. For Gaussian statistics, Skewness is 0 and Kurtosis is 3.

A plot of spectral broadening of the sum frequency intensity spectra is also included in Fig. 17. The reproducibility for the measurements is not as great as for the pressure measurements. Nonetheless, broadening is low at the edges of the jet and increases towards the axis. The profile is somewhat symmetric, which along with the shape of the profile, suggests velocity dependence of the broadening.

A progression of scattered sum frequency intensity spectra across the jet is presented in Fig 18. These waveforms are related to the velocity probability distributions across the jet, although the exact correlation is not known.

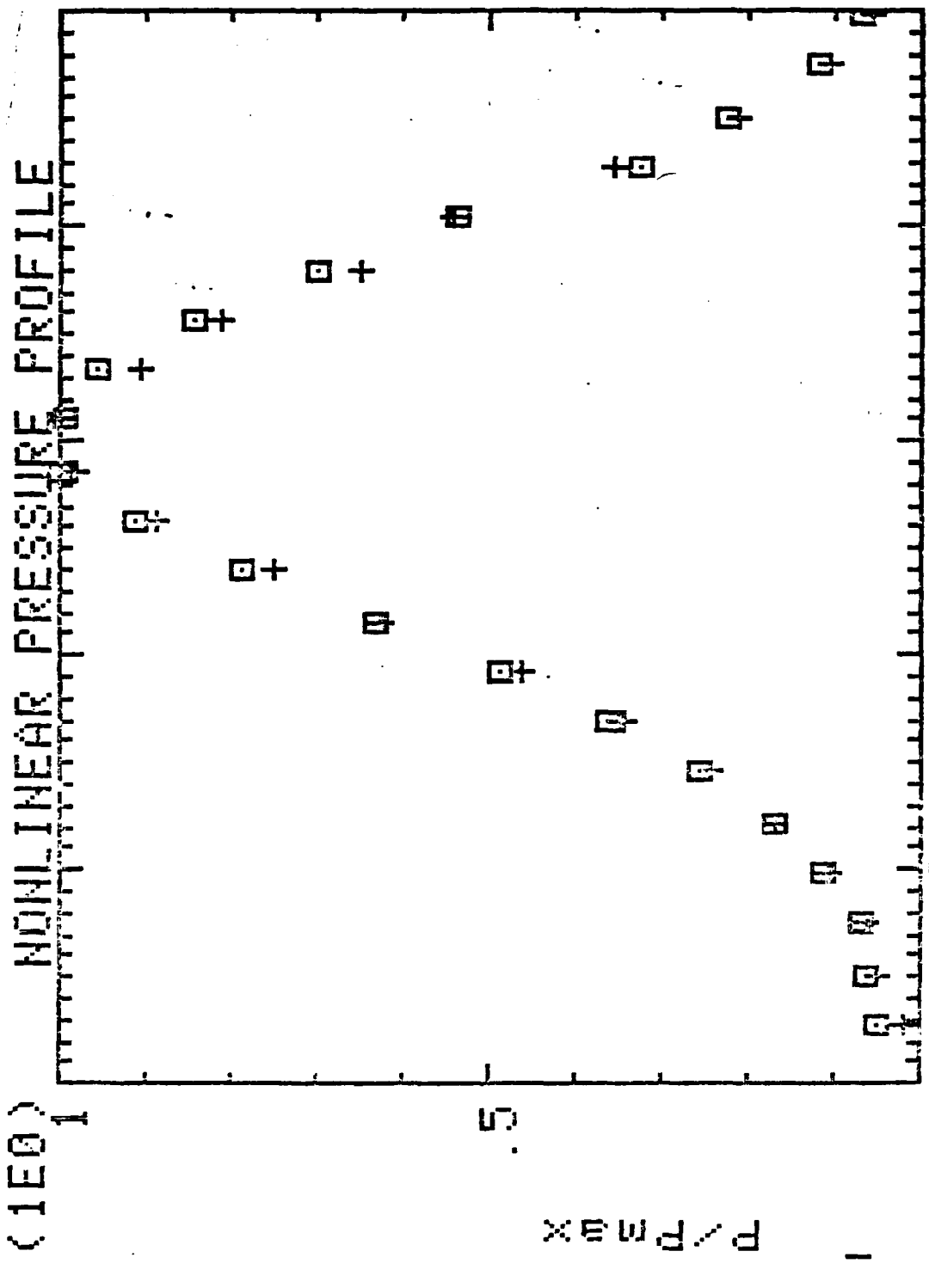

Fig 15: Nonlinear pressure profiles using high resolution frequency sampling
(Data points corresponding to two different data runs)

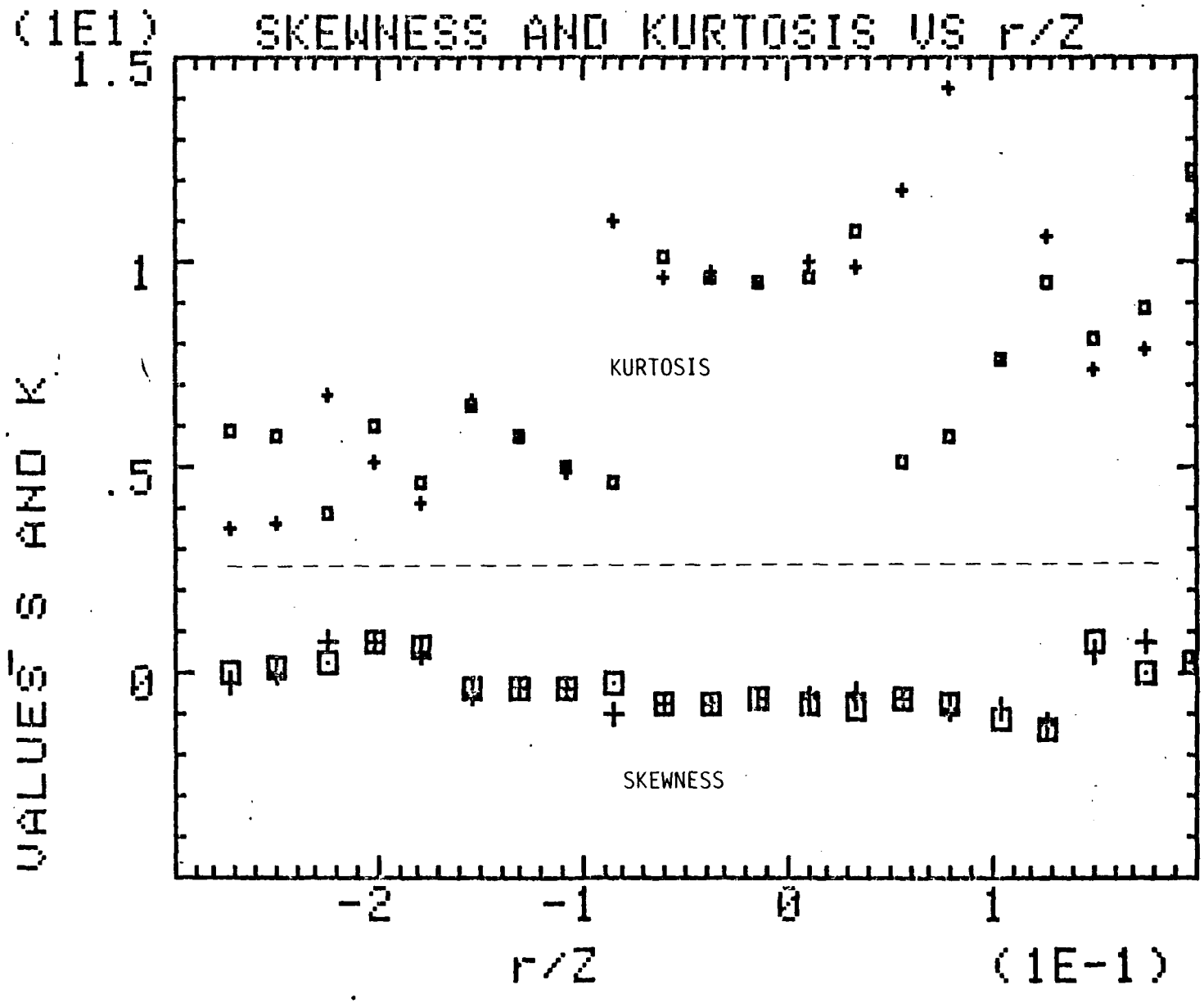

Fig 16: Nonlinear Skewness and Kurtosis Profiles from high resolution frequency scanning
(Data points corresponding to two different data runs)

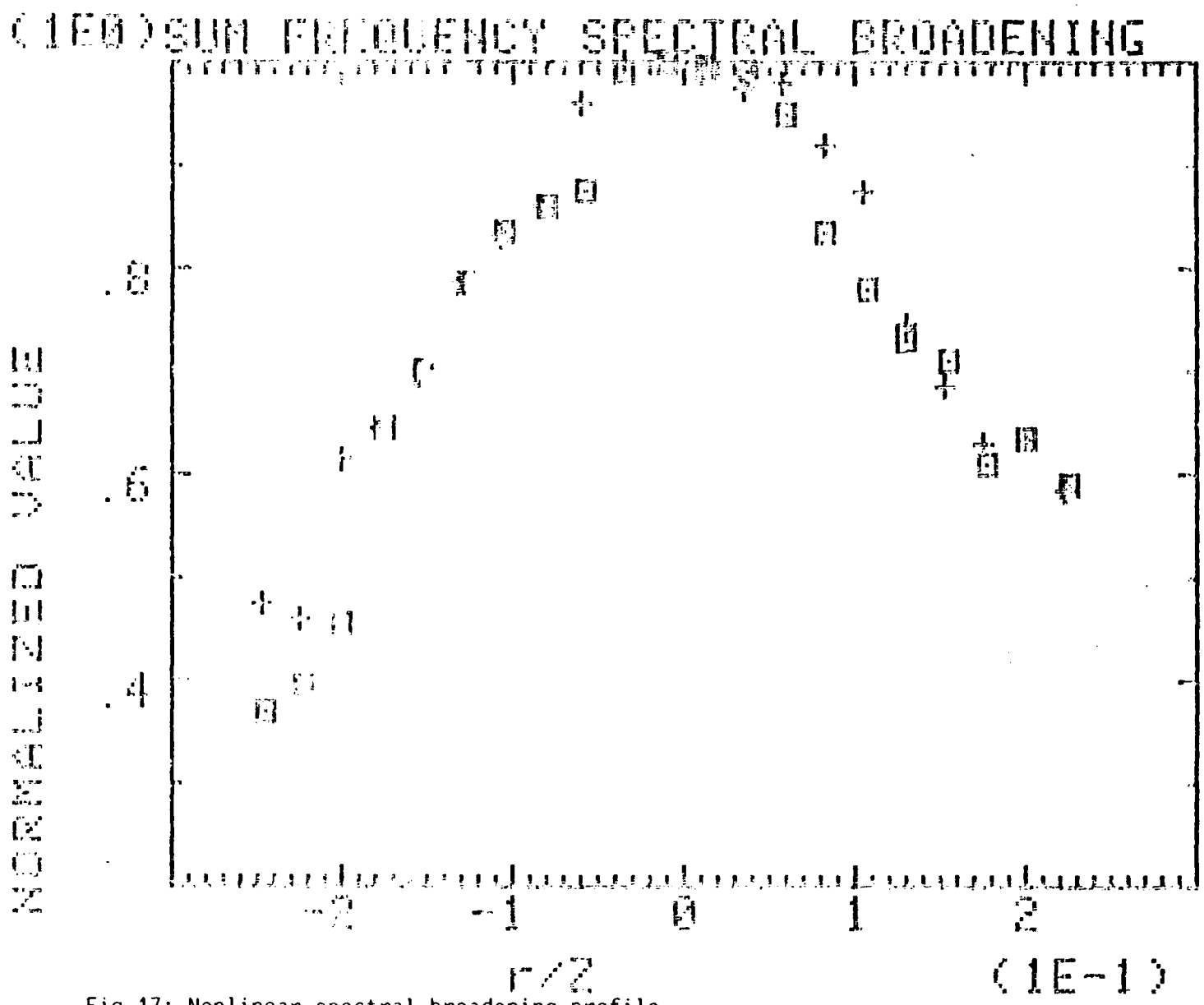

Fig 17: Nonlinear spectral broadening profile
(Data points corresponding to two different data runs)

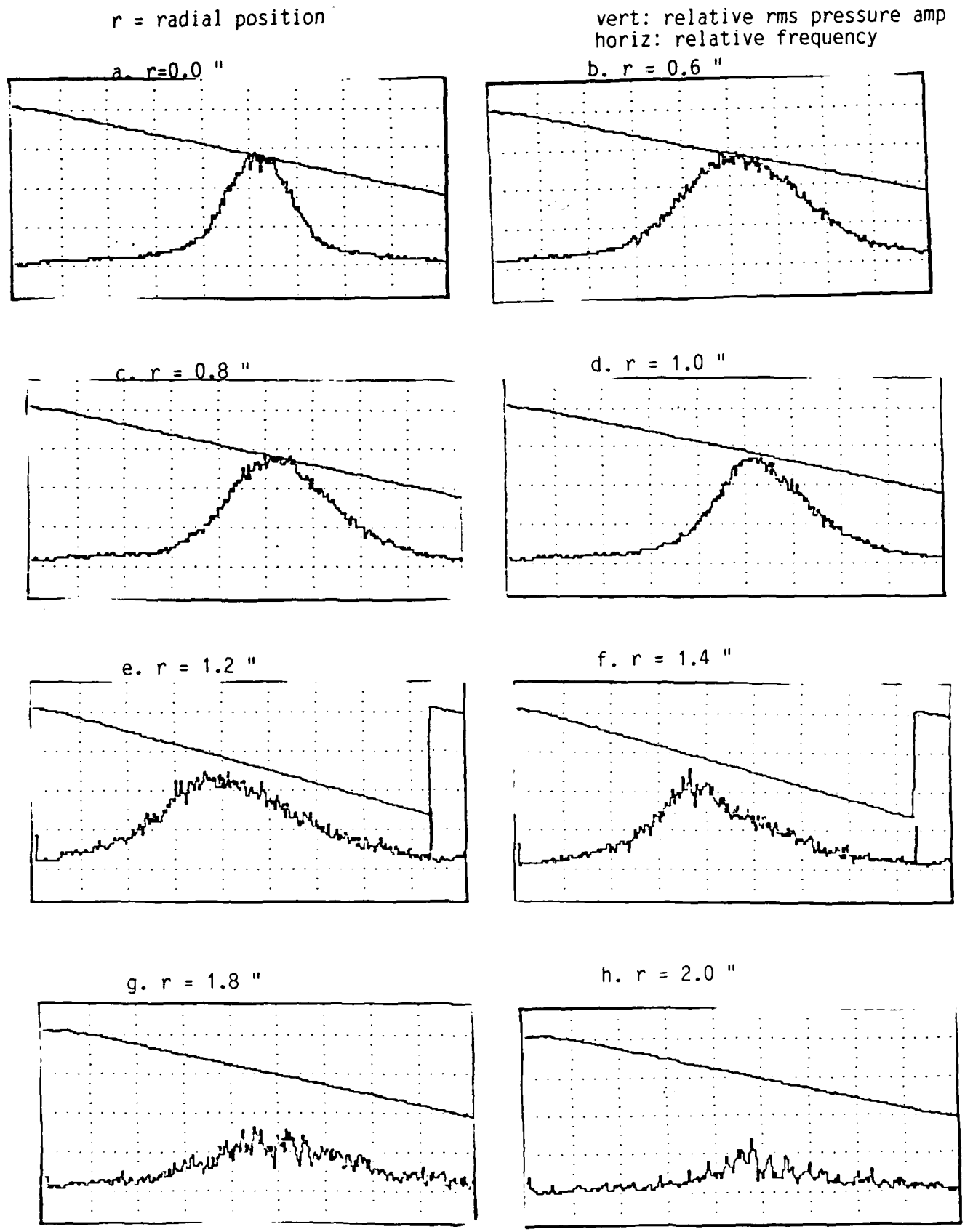

Fig 18: Progression of sum frequency spectra from the axis to the edge of the jet

SINGLE BEAM SCATTERING RESULTS

Scattering results of the 1.95 MHz beam from the interaction volume are presented here in order to make comparisons with the nonlinear scattering.

A progression of scattered single beam spectra across the width of the jet is shown in Fig 19. Fig 20 shows plots of Skewness and Kurtosis profiles for two data runs using the intensity spectra. Both Skewness and Kurtosis profiles show symmetry about the center of the jet and are continuous curve forms. The Skewness, a measure of symmetry of the single beam spectra, is close to 0, a value representing symmetry, at the center of the jet and increases at the edges. The Kurtosis is relatively low at the center of the jet and increases at the edges. At the center, though, the values of Kurtosis are higher than the values gotten for positions further from the center. This result is similar to that obtained for the nonlinear scattered spectra as shown in Fig 21. Except for that case, a sharp drop in Kurtosis is realized at r/Z = + or - .6. Also the Kurtosis values for the sum frequency scan are much higher at the center. Thus the nonlinear scattering seems to amplify this Kurtosis value at the center of the jet. The nonlinear data also show increases in Skewness and Kurtosis at the edges of the jet which agrees with linear results.

The single beam root mean square pressure profile shown in Fig. 22 is broader than the nonlinear scan. This is reflected by the constants obtained from a curve fit of the data.(See Table 1). The spatial resolution of the linear scattering is suspected to be less than the spatial resolution of the scattered sum frequency, because the scattering volume of the single beam is

not as well defined as the scattering volume of the crossed beams.

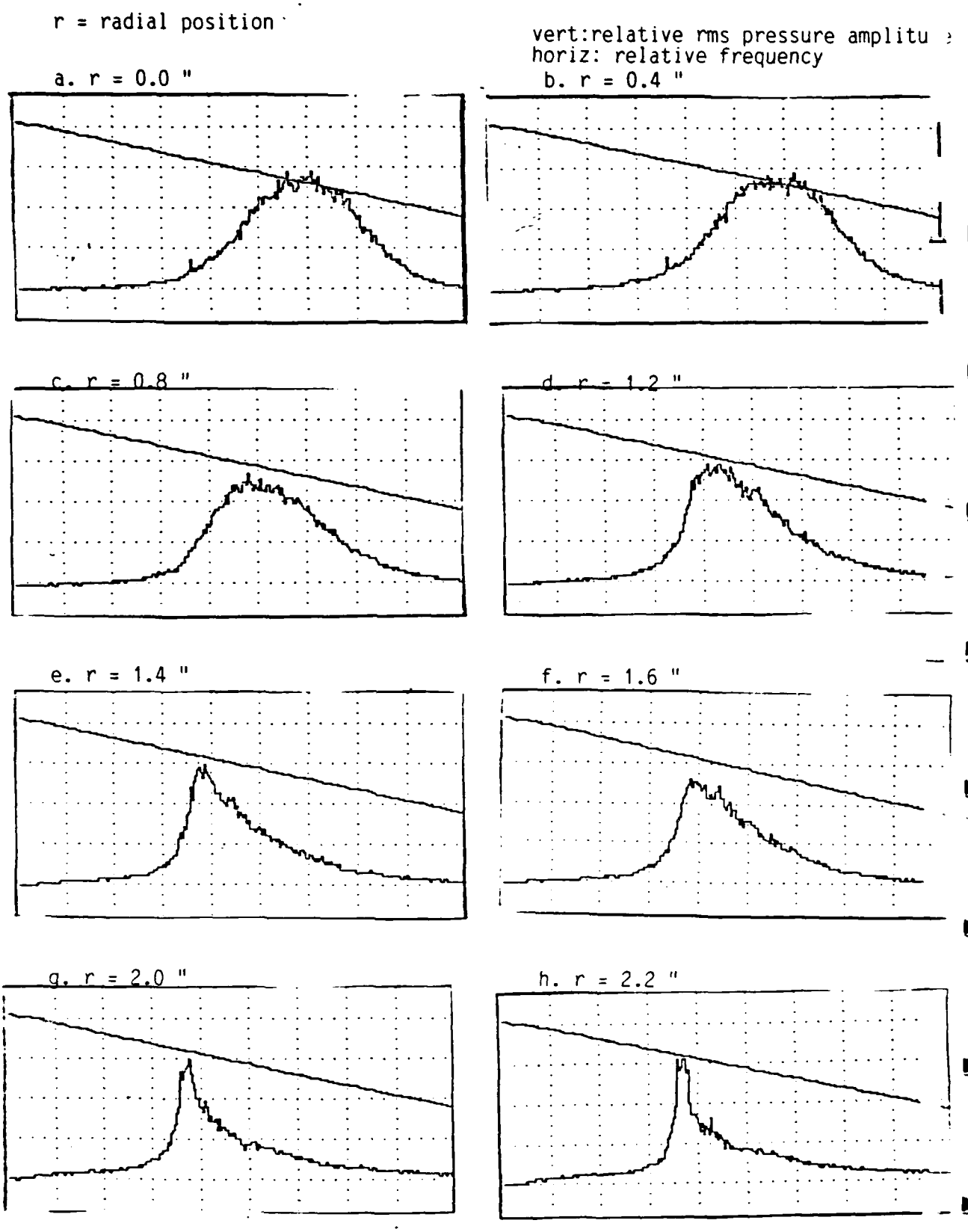

Fig 19: Progression of scattered single beam (1.95 MHz) spectra from the axis to the edge of the jet

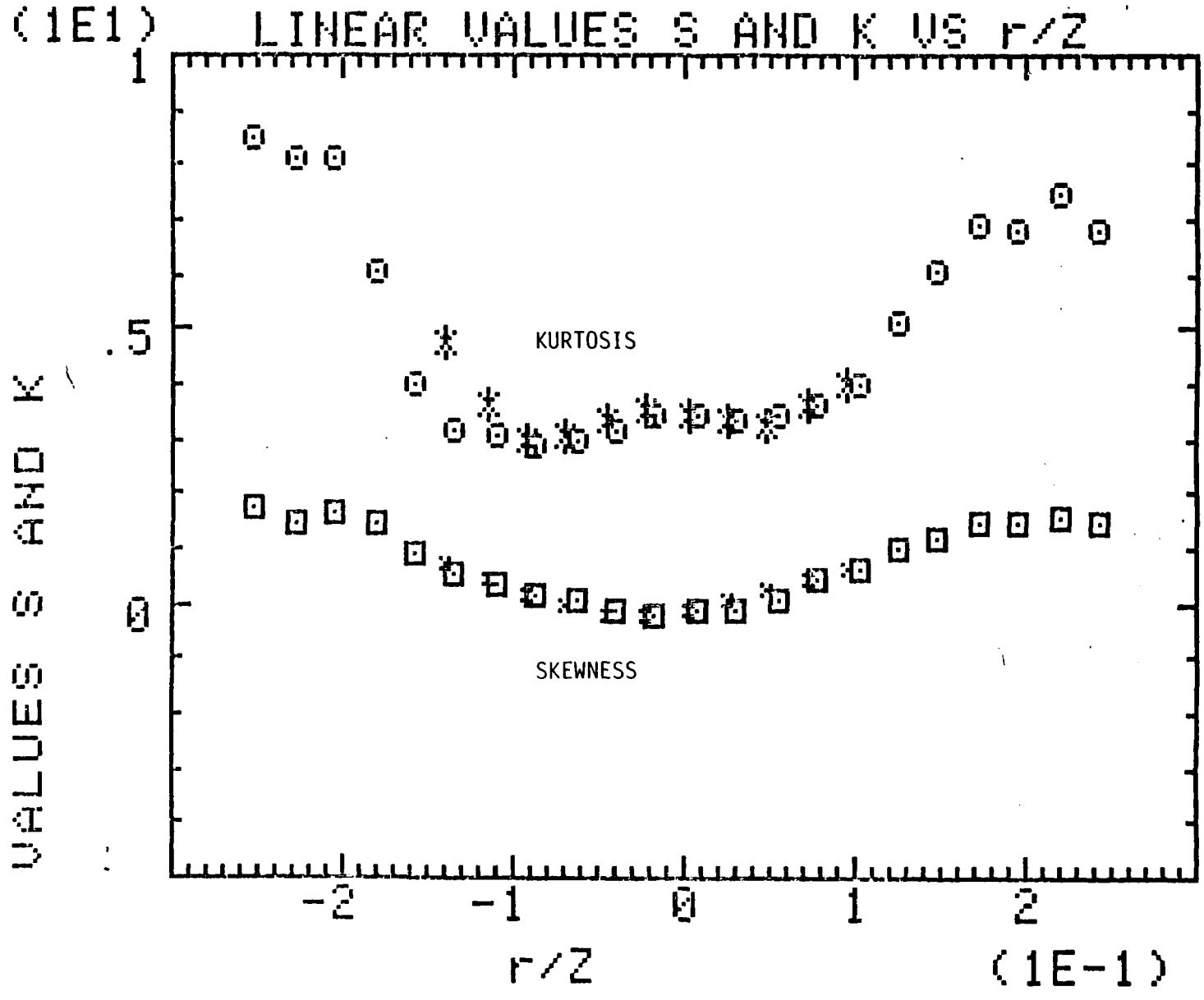

Fig 20: Single beam Skewness and Kurtosis profiles
(data points corresponding to two different data runs)

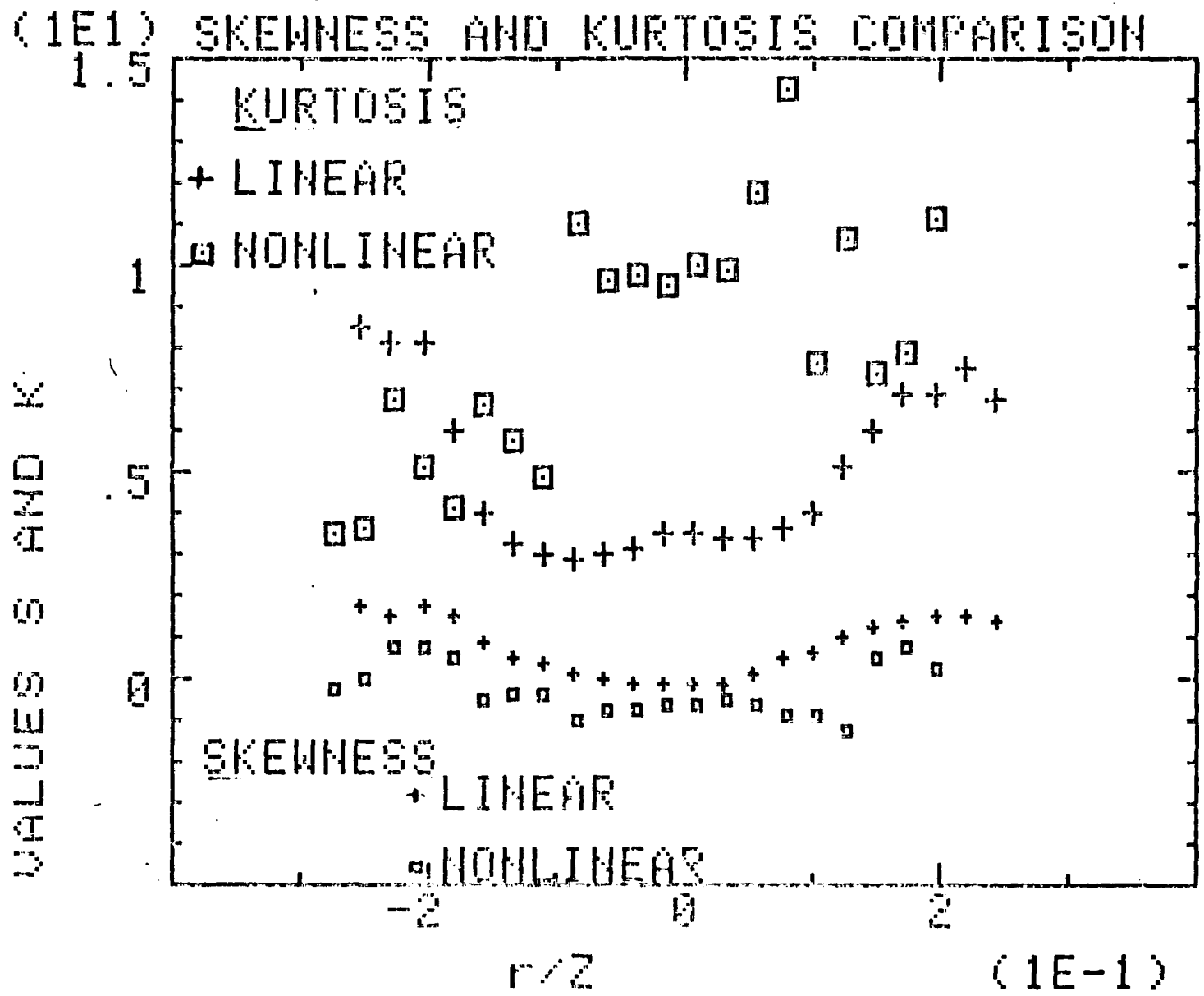

Fig 21: Comparison of Skewness and Kurtosis for nonlinear vs single beam scattering

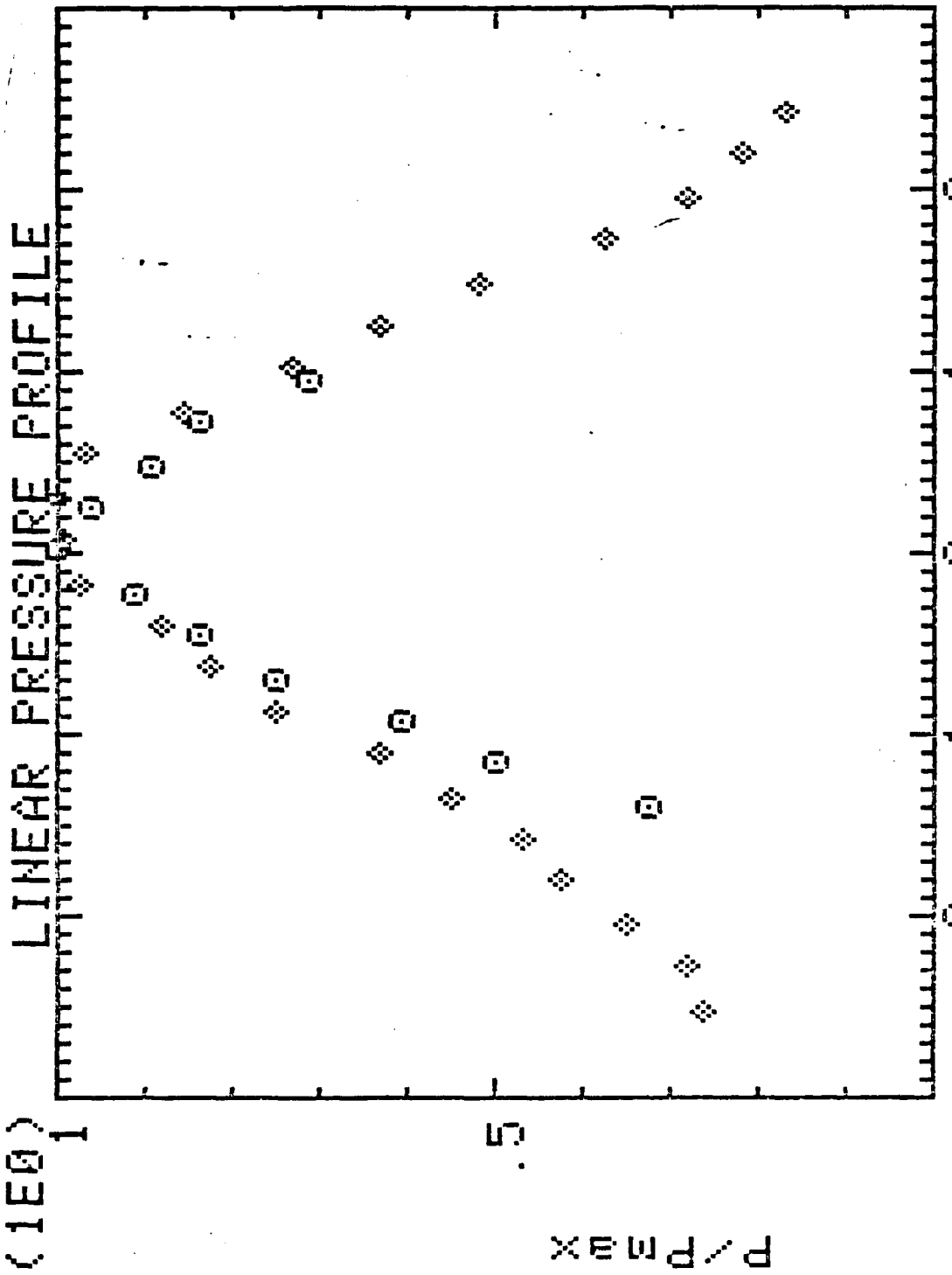

Fig 22: Single beam pressure profiles
(data points corresponding to two different data runs)

CONCLUSIONS

Trends in the curve fitted constants of scattered pressure profiles show correlation with the curve-fitted constants of turbulent velocity profiles of other researchers, not mean velocity profiles, even though mean velocities are on average three times as large as turbulent velocities. Thus, the scattering mechanism of the sum frequency sound beam is the interaction of acoustic velocities with turbulent velocities.

The sum frequency and single beam spectra are seen to change across the width of the turbulent jet. Both are suspected to match turbulent velocity probability distributions although none of these experimentally determined distributions were found in the literature with which to compare the acoustic spectra. In addition Doppler shift calculations from the spectra measure the mean flow in the interaction region. Thus, the crossed beam arrangement by describing the turbulent and mean velocities in the flow can fully map out the turbulent fluid field.

Few other instruments are currently available to scientists for fully mapping out turbulent flow. The results presented here show the crossed focussed beam arrangement is another diagnostic tool to measure turbulence with advantages of ruggedness and negligible disturbance of the fluid field.

Although the sum frequency scattering has been shown to be due to turbulent fluctuations, the role which the turbulent velocity components play, as given by Lighthill 's Stress Tensor, is not conclusive, and is grounds for future angular measurements of scattering.

Bubbles entrailed in the flow seemed to track the flow and were

necessary to detect the nonlinear scattered sum frequency. The bubbles have an amplification effect on the sum frequency scattered intensity.

The results presented herein show that the development of the crossed beam arrangement as an effective turbulence measuring instrument has been realized. The arrangement built in the past year will be fine tuned and used for various further scattering measurements and refining of results in the near future. The arrangement is new and further measurements are needed to fully understand its capabilities for mapping out turbulent fluid fields.

ACKNOWLEDGEMENTS

The author would first like to thank his Trident advisor, Prof. Murray Korman, who introduced the idea of a focussed crossed beam arrangement. In addition, he supervised its construction, measurements, and interpretation of results, and always had other alternatives for the frequent inadequacies and malfunctions with the experimental equipment. Prof. Paul Uldrick, co-advisor for the project, is also appreciated for his support.

Much of the construction of the arrangement was completed using the expertise and muscle of the technical support personnel from the Physics department. Charlie Holloway was especially helpful for frequent alterations to the design.

Major components in the construction were built by the Engineering Technical Support Personnel under the guidance of Carl Owen and John Smaltz.

Technical Services Division helped extensively with the plumbing design and donated the pump. Most other plumbing parts were donated from surplus at the pipe shop, Perry Center, USNA, while other parts were donated by the Oceanography Department.

Additionally, the author would like to recognize the Naval Academy faculty members who helped with various questions. Prof. Granger, Prof. Nordling, Prof Shelby, and the CADIG staff willingly volunteered their expertise in their various fields.

Two other students, Dan Magsig, and Midn 1/c Mary Jackson helped with the project throughout. Dan's computer programming was much

appreciated, and many of the measurements required Mary's help.

The author would also like to thank Marge Bem, Anna Svensson, and Paul Hanover, for helping on various typing assignments, and lastly recognizes NARC for its funding of the project.

BIBLIOGRAPHY

1. Corrsin, S, and M. S. Uberoi: National Advisory Comm. Aeronaut. Tech. Notes No 1863.

2. Corrsin, S, and M. S. Uberoi: National Advisory Comm. Aeronaut. Tech. Notes No 2124.

3. Corrsin, S, and A. L. Kistler: National Advisory Comm. Aeronaut. Tech. Notes No 3133.

4. Hinze, J. O., 1959 Turbulence, McGraw-Hill, New York, 586 pp.

5. Hinze, J. O. and Zijnen, B. G. Van der Hegge, 1949. Transfer of heat and matter in the turbulent mixing zone of an axially symmetrical jet. J. Appl. Sci. Res. A1:435-461.

6. Ishimaru, Wave Propagation and Scattering in a Random Medium, (Academic Press, New York, NY, 1978), Vol. 1, Ch. 4 and Vol. 2, Ch. 16.

7. Korman, M. S. and Beyer, R. T., "The Scattering of Sound by Turbulence in Water, "J. Acoust. Soc. Am 67, 1980-1987 (1980).

8. Korman, M. S., "Experiments on the Scattering of Sound by Turbulence," Ph.D. Thesis, Brown University, 1981.

9. Korman, M. S. and Beyer, R. T., "Nonlinear Scattering of Crossed Ultrasonic Beams in the Presence of Turbulence in Water. Part I. Experiments," submitted to J. Acoust. Soc. Am. (1987).

10. Kraichnan, R. H., "The Scattering of Sound in a Turbulent Medium," J. Acoust. Soc. Am. 25, 1096-1104 (1953).

11. Kraichnan, R. H., "The Scattering of Sound in a Turbulent Medium," J. Acoust. Soc. Am., 25, 1096-1104 (1953); erratum 28, 314 (1956).

12. Kraichnan, R. H., "The Scattering of Sound in a Turbulent Medium," J. Acoust. Soc. Am. 25, 1096-1104, (1953).

13. Lighthill, M. J., "On Sound Generated Aerodynamically," Proc. Roy. Soc. (LONDON) I. A211, 564-587 (1952); II A222, 1-32 (1954).

14. Lighthill, M. J., "On Energy Scattered from the Interaction of Turbulence with Sound or Shock Waves," Proc. Camb. Phil. Soc., 49 531-551 (1953).

15. Panchev, S., "Random Functions and Turbluence," Copyright 1971 S. Panchev.

16. Pope, S. B., Phys. Fluids, 24, 588 (1981).

17. Tennekes, H., and Lumley, J. L., A First Course in Turbulence, Copyright 1972 by the Massachussetts Institute of Technology.

18. Westervelt, P. J., "Scattering of Sound by Sound, J. Acoust. Soc. Am. 29, 199-203 (1957).

19. Westervelt, P. J., "Scattering of Sound by Sound," J. Acoust. Soc. Am. 29, 934-935 (1957).

20. Wygnanski, I., and Fiedler, H., J. Fluid Mech., 38, 577 (1969).

21. Wygnanski, I., and Fiedler, H. E., J. Fluid Mech., 41, 327 (1970).

22. Wygnanski, I., and Fiedler, 1969. Some measurements in the self-preserving jet. J. Fluid Mech., 38:577-612.

23. Zijnen, B. G., Van der Hegge, 1958a, Measurements of the velocity distribution in a plane turbulent jet of air. Apl. Sci. Res., Sect. A, 7:256-276.

24. Zijnen, B. G.,Van der Hegge, 1958b. Measurements at turbulence in a plane jet of air by the diffusion method by the hot wire method. Appl. Sci. Res., Sect. A, 7:293-313.

APPENDIX A: SUPPORTING STRUCTURE

In order to align and to keep the crossed sound beams aligned, heavy duty rotating and travelling mechanisms were assembled to position the sending and receiving transducers (see Fig. 23). Aligning the acoustic beams involved using a pulse-echo technique. In a pulse echo alignment (shown in Fig. 24), a single transducer both sends and receives a sound pulse. The sound pulse transmitted by the transducer, bounces off a solid object in its path and returns to the same transducer, where the returned signal strength can be detected. The solid object used for the pulse-echo alignment is a 2 mm diameter stainless steel bead, suspended in the water and located in the planned interactive region. By maximizing the received echo amplitude the transducer is aligned. The bead is removed from the water after alignment of all three transducers.

A compound slide table with an 8 inch travel guides the fixed transducers across the width of the jet and marks position. Another alignment problem required the axis of the water jet to be parallel to the ground. A machined square metal block is fitted over the nozzle. The plenum to which is connected the nozzle is then shimmed so that the front edge of the metal block aligns with a hanging string. The tracks of the carriage must also scan perpendicular to the jet axis. A dial indicator was used to adjust the travel alignment. Once all the transducers are aligned with the generated turbulent water jet, and sending and receiving electronics are constructed, scans of the jet can be accomplished.

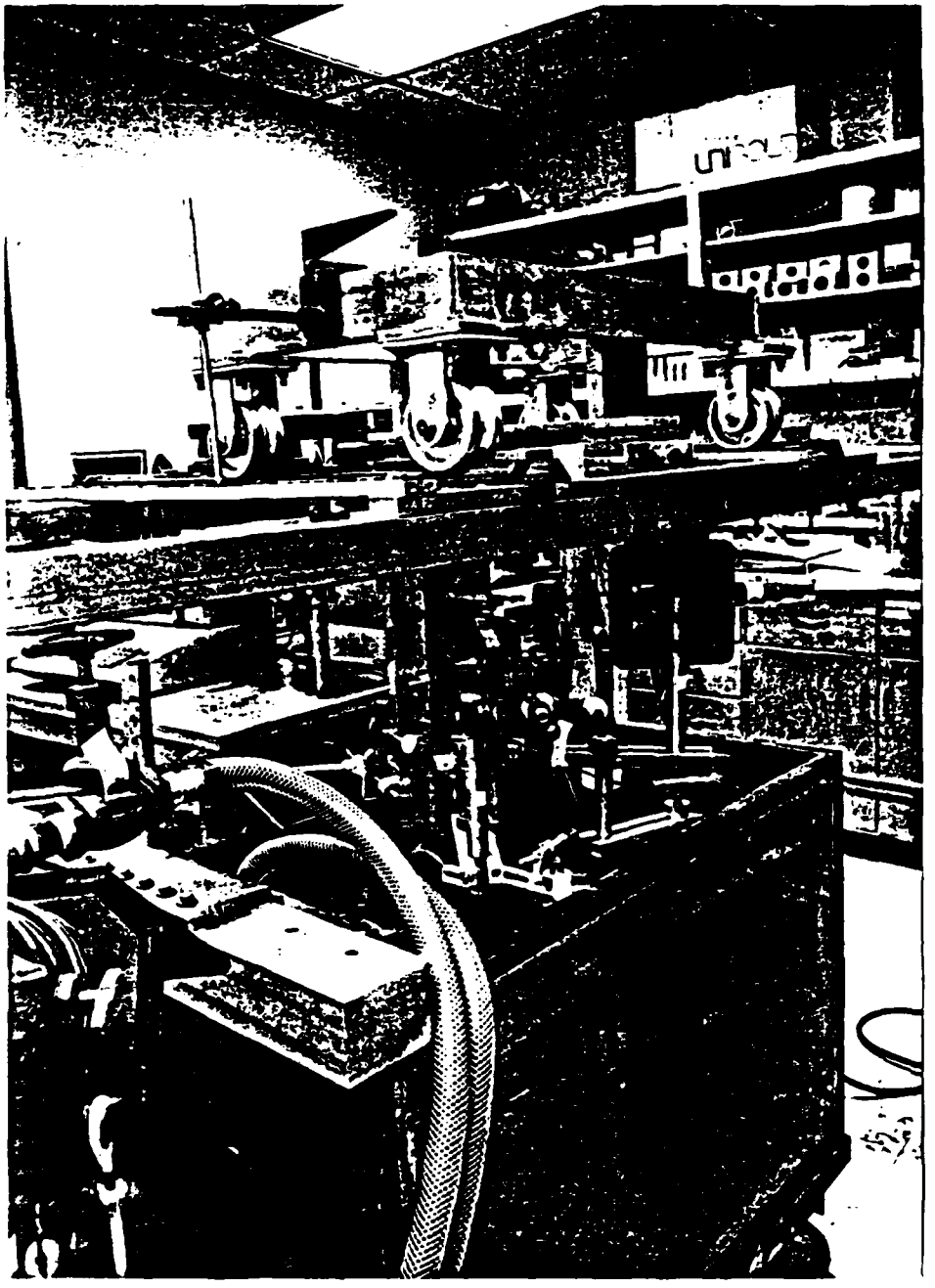

Fig 23: Positioning equipment and supporting structure

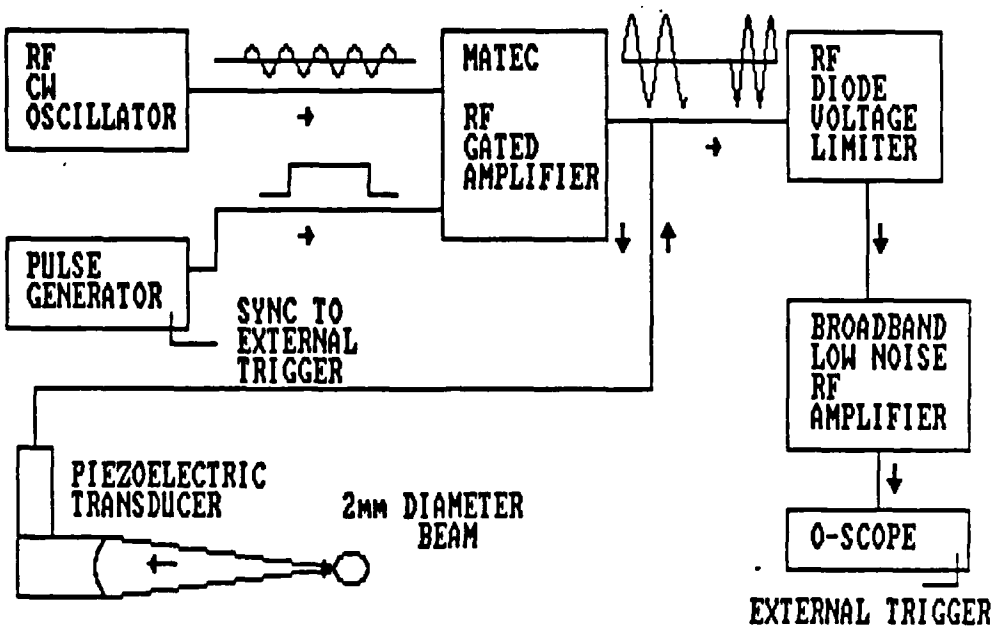

FIG.24: PULSE-ECHO ELECTRONICS

APPENDIX B: DATA FIT COMPARISON OF PRESSURE PROFILES TO PUBLISHED VELOCITY PROFILES

This section presents in tabular form, curve fitting constants calculated for four curve forms applied to pressure profiles and published mean and turbulent velocity profiles. The curve forms chosen have been used successfully in the past to fit mean and turbulent velocity measurements. The purpose of this section of results is to correlate the scattered sum frequency pressure profiles to turbulent or mean velocity profiles to show conclusively which causes the scattering of the sum frequency sound beam.

The curve forms chosen are :

1) $Y = \exp(A\eta^2)$

2) $Y = \exp(A\eta^2 + B\eta^4)$

3) $Y = 1/(1+A\eta^2)^2$

4) $Y = \mathrm{sech}^2(\delta x/z)$

where Y= u'/u'max, U/Umax, P/Pmax.

Velocity data is taken from the published plots of Corrsin, Wygnanski, and Reichardt. Their experimental results have been digitized from published plots using the CADIG facilities at the Naval Academy. This data was then manipulated into a consistent form. The curve fitting methodology is based on linearizing the equations and using a least squares fit to solve for the coefficients.

Table 1, gives the constants fitted to all four curve forms for all the velocity and pressure profiles investigated. For curve form 1, the turbulent velocity constants all

range from -35 to -56, while the mean velocity constants are more negative and range from -54 to -82. Comparison of the constants of the pressure data which range from -41 to -48 indicate the scattered sum frequency pressure is proportional to the turbulent velocity, not the mean velocity in the flow. This achieves one main objective in the study -- to discover the scattering mechanism of the sum frequency. That mechanism is found to be a mixing of sound velocity with turbulent velocity, not mean velocity.

Curve form 2 has two constants, with one being a correction factor to the first, thus making these fits hard to compare because of the wide variations between constants.

Results for curve form 3, like results for curve form 1, support the conclusion of a turbulent scattering mechanism. The range of mean velocity constants for curve 3, 55-135, are higher than acoustic constants, 41-57, which again correlate with turbulent velocity profiles which range from 21 to 64. Lastly, the fits to curve form 4, also support the turbulent scattering discovery. The acoustic constants range from 8.7 to 9.8, correlating with turbulent velocity constants, 6.7 to 9.9. The mean velocity constants are higher at 9.8 to 12.5. Graphical fits comparing pressure profiles to mean and turbulent profiles are shown in Figs. 25 and 26.

In addition to the mean velocity profiles obtained from published data, a mean velocity profile is presented from pitot tube measurements made across the jet at 30 nozzle diameters from the outlet. This data is also presented in the table and used for the correlational study. The profile is plotted in Fig 27. From the plot, the profile is seen to be symmetric about the axis of the jet and continuous. This ensures the jet created for this study matches jets used in the studies with which the acoustic pressure correlates.

Table 1

ACOUSTIC PRESSURE FITS

Equation $\rho = \frac{r}{x-3d}$	Constant	Nonlinear Pressure				Standard Deviation		Linear	
		Jan 26	Feb 23	Mar 1	Mar12	Mar 1	Mar 12	Mar 16	Mar 22
1. $Y = e^{(A\rho^2)}$	A	-48.04	-47.46	-41.31	-45.39	-12.54	-10.72	-43.81	-22.36
2. $Y = e^{(A\rho^2 B\rho^4)}$	A	-47.64	-71.59	-61.63	-57.68	-13.29	-13.16	-35.96	-29.2
	B	- 6.3	339.4	313.9	190.4	13.99	45.97	-446.7	116.25
3. $Y = \frac{1}{(1 + A\rho^2)^2}$	A	51.85	57.47	41.13	51.13	7.67	6.20	27.5	15.73
4. $Y = \mathrm{sech}^2(\frac{\sigma r}{z})^2$	σ	9.200	9.853	8.7029	9.174	4.160	3.825	7.68	5.84

TURBULENT VELOCITY (RMS) FITS

		Wygnanski				Corrsin			
1.	A	-35.45	-42.88	-53.43	-56.67	-46.67	-43.86	-58.92	-35.2
2.	A	-20.70	-20.39	-16.79	-43.99	-34.84	-1.015	-41.35	-15.77
	B	-695.6	-598.8	-843.4	-321.4	-290.5	-1166	-414.3	-388.7
3.	A	21.9	34.9	59.6	54.95	40.7	34.73	63.53	32.52
4.	σ	6.723	7.758	8.849	9.623	8.389	8.243	9.910	6.712

MEAN FLOW DATA CURVE FITS

		Corrsin				Reichardt	
1.	A	-68.67	-76.17	-77.66	-82.08	-81.68	-54.1
2.	A	-79.14	-72.42	-67.74	-62.59	-49.23	-69.7
	B	401.4	-152.6	-397.8	-456.6	-778.18	32.8
3.	B	55.94	66.65	68.11 50.84	135.3	158	55.08
4.	σ	10.50	11.00	10.88	12.49	12.32	9.838

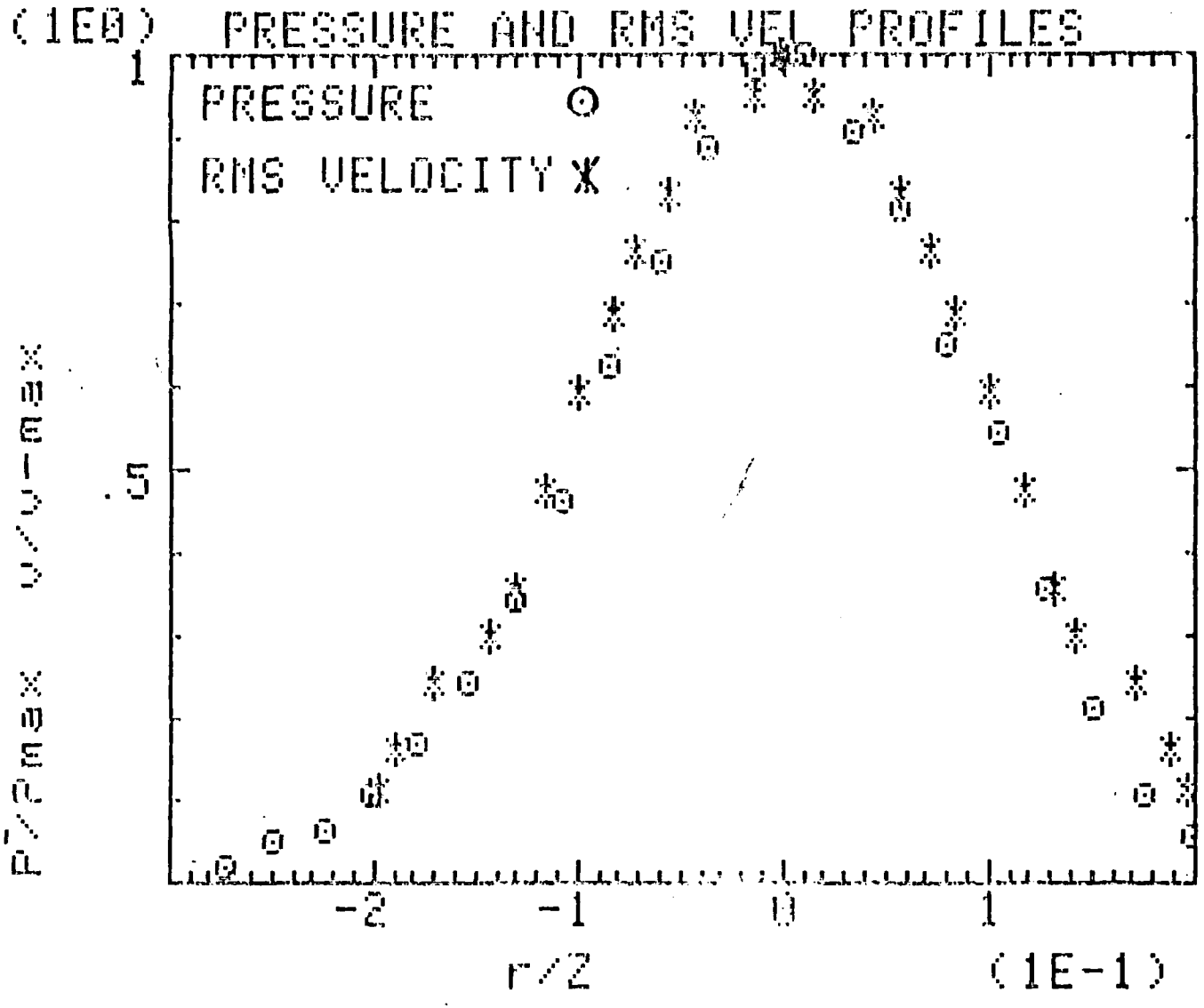

Fig 25: Comparison of nonlinear scattering pressure profile to RMS velocity profile

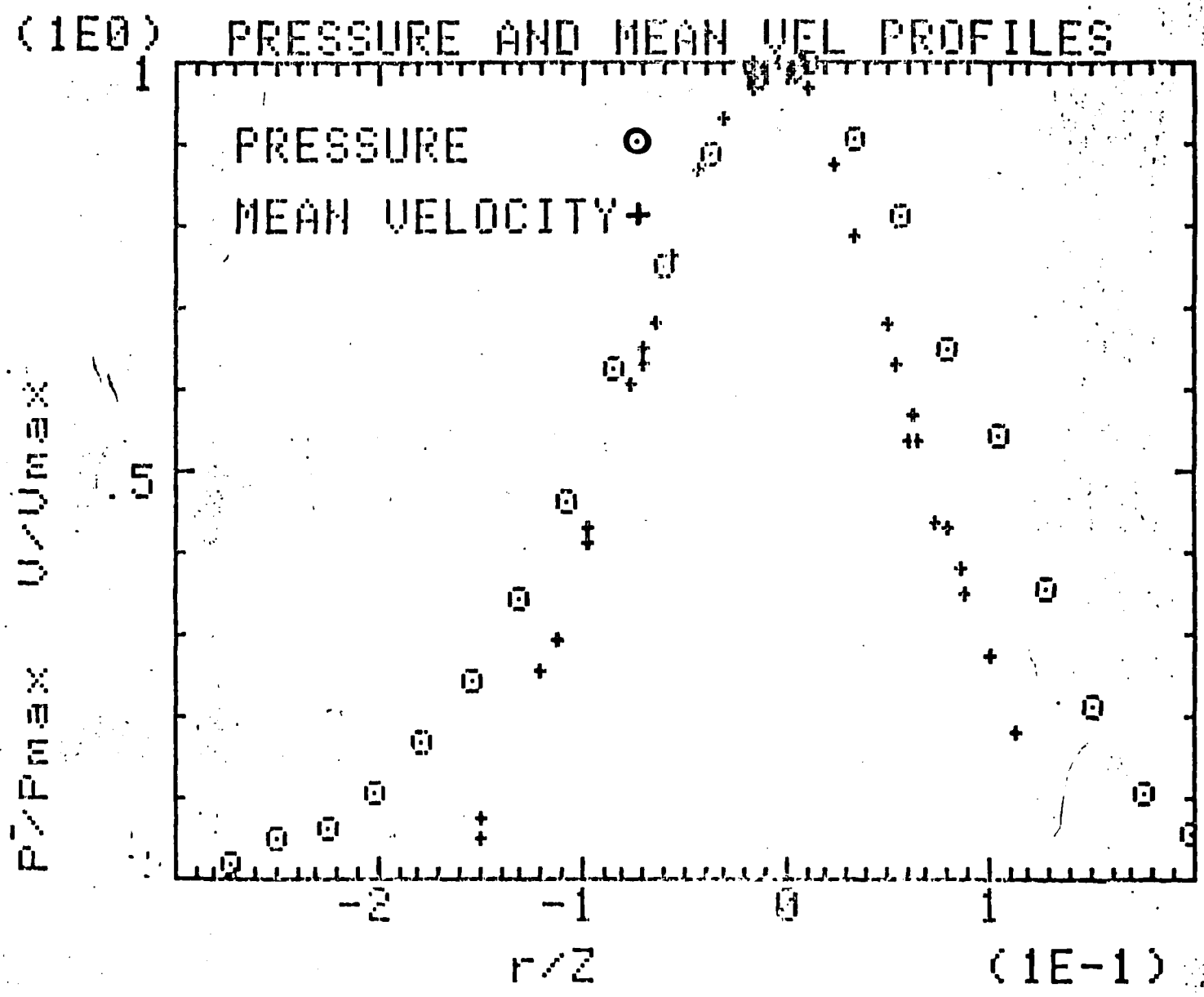

Fig 26: Comparison of nonlinear pressure profile to mean velocity profile

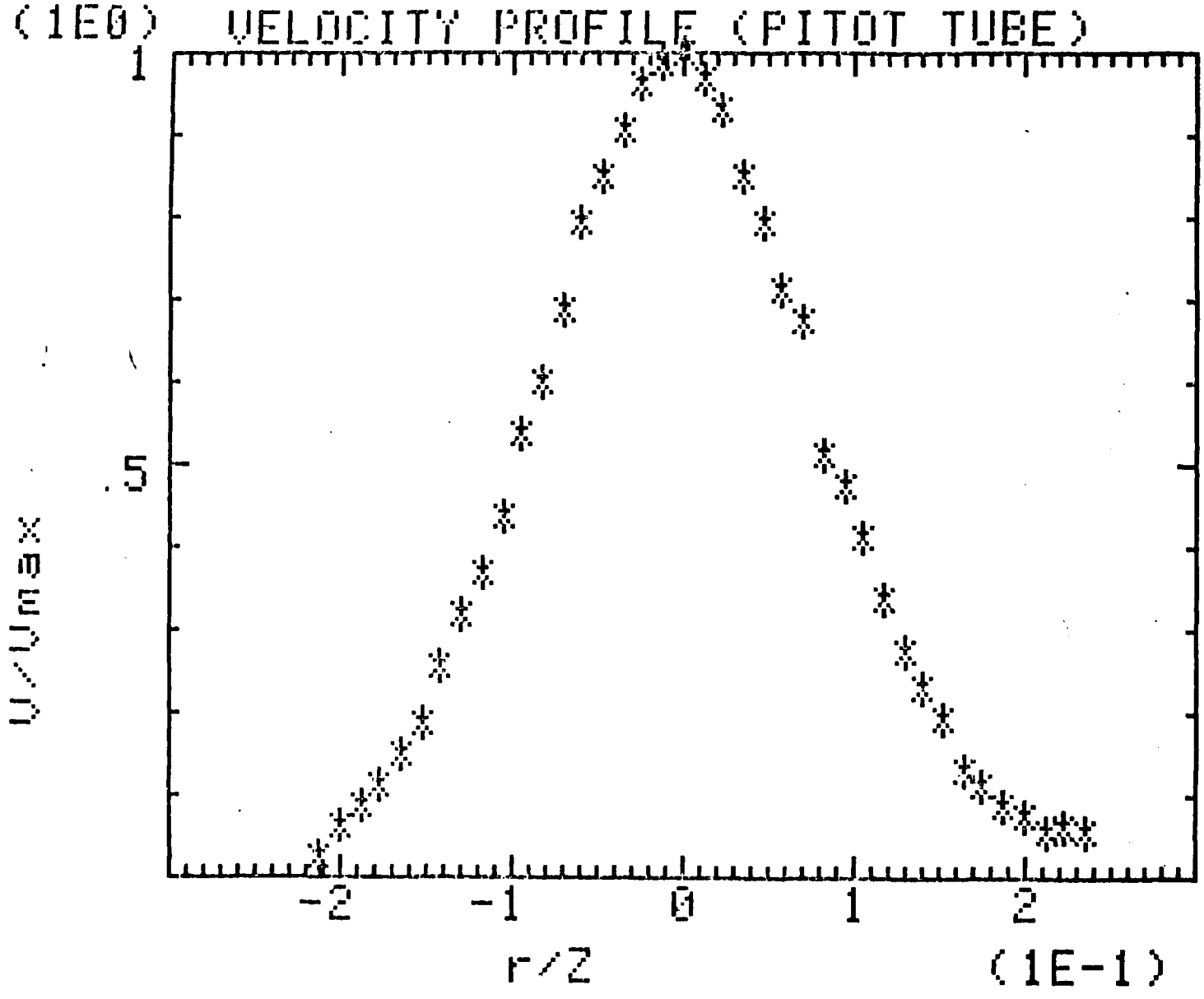

Fig 27: Mean velocity profile from pitot tube measurements